Article

Current Biology

Genomics of New Ciliate Lineages Provides Insight into the Evolution of Obligate Anaerobiosis

Highlights

- Discovery and cultivation of two new classes of marine ciliates thriving in anoxia
- Phylogenomics reveals a major clade of obligate anaerobes in ciliates
- Novel insights into evolution of mitochondrial metabolism in anaerobic eukaryotes
- Transitions to obligate anaerobiosis might be facilitated by prokaryotic symbionts

Authors

Johana Rotterová, Eric Salomaki, Tomáš Pánek, ..., Roxanne A. Beinart, Martin Kolísko, Ivan Čepička

Correspondence

johana.rotterova@natur.cuni.cz

In Brief

Numerous eukaryotes have switched to anaerobiosis, variously reducing their mitochondrial metabolism. Rotterová et al. describe two new classes of obligately anaerobic ciliates with prokaryotic symbionts and reduced mitochondria with unique pathways for energetic metabolism, introducing possible mechanisms of transitions to obligate anaerobiosis.

Rotterová et al., 2020, Current Biology *30*, 1–14
June 8, 2020
https://doi.org/10.1016/j.cub.2020.03.064

CellPress

Please cite this article in press as: Rotterová et al., Genomics of New Ciliate Lineages Provides Insight into the Evolution of Obligate Anaerobiosis, Current Biology (2020), https://doi.org/10.1016/j.cub.2020.03.064

Current Biology
Article

Genomics of New Ciliate Lineages Provides Insight into the Evolution of Obligate Anaerobiosis

Johana Rotterová,[1,8,*] Eric Salomaki,[2] Tomáš Pánek,[1] William Bourland,[3] David Žihala,[4] Petr Táborský,[2] Virginia P. Edgcomb,[5] Roxanne A. Beinart,[6] Martin Kolísko,[2,7] and Ivan Čepička[1]
[1]Department of Zoology, Faculty of Science, Charles University, Prague 128 43, Czech Republic
[2]Institute of Parasitology, Biology Centre Czech Academy of Sciences, České Budějovice 370 05, Czech Republic
[3]Department of Biological Sciences, Boise State University, Boise, ID 83725-1515, USA
[4]Department of Biology and Ecology, Faculty of Science, University of Ostrava, Ostrava 710 00, Czech Republic
[5]Department of Geology and Geophysics, Woods Hole Oceanographic Institution, Woods Hole, MA 02543, USA
[6]Graduate School of Oceanography, University of Rhode Island, Narragansett, RI 02882, USA
[7]Department of Molecular Biology and Genetics, Faculty of Science, University of South Bohemia, 370 05 České Budějovice, Czech Republic
[8]Lead Contact
*Correspondence: johana.rotterova@natur.cuni.cz
https://doi.org/10.1016/j.cub.2020.03.064

SUMMARY

Oxygen plays a crucial role in energetic metabolism of most eukaryotes. Yet adaptations to low-oxygen concentrations leading to anaerobiosis have independently arisen in many eukaryotic lineages, resulting in a broad spectrum of reduced and modified mitochondrion-related organelles (MROs). In this study, we present the discovery of two new class-level lineages of free-living marine anaerobic ciliates, Muranotrichea, cl. nov. and Parablepharismea, cl. nov., that, together with the class Armophorea, form a major clade of obligate anaerobes (APM ciliates) within the Spirotrichea, Armophorea, and Litostomatea (SAL) group. To deepen our understanding of the evolution of anaerobiosis in ciliates, we predicted the mitochondrial metabolism of cultured representatives from all three classes in the APM clade by using transcriptomic and metagenomic data and performed phylogenomic analyses to assess their evolutionary relationships. The predicted mitochondrial metabolism of representatives from the APM ciliates reveals functional adaptations of metabolic pathways that were present in their last common ancestor and likely led to the successful colonization and diversification of the group in various anoxic environments. Furthermore, we discuss the possible relationship of Parablepharismea to the uncultured deep-sea class Cariacotrichea on the basis of single-gene analyses. Like most anaerobic ciliates, all studied species of the APM clade host symbionts, which we propose to be a significant accelerating factor in the transitions to an obligately anaerobic lifestyle. Our results provide an insight into the evolutionary mechanisms of early transitions to anaerobiosis and shed light on fine-scale adaptations in MROs over a relatively short evolutionary time frame.

INTRODUCTION

Anaerobic eukaryotes have long intrigued biochemists and evolutionary biologists, as free oxygen is widely considered essential for life in this domain. Among other functions in the cell, oxygen plays a crucial role as a terminal electron acceptor in mitochondrial ATP production via oxidative phosphorylation. Yet numerous eukaryotic lineages have adapted to low-oxygen concentrations and thrive in hypoxic or even anoxic environments [1]. Although some of them are still able to survive exposure to oxygen, others are obligate anaerobes whose mitochondria have been reduced to various forms of mitochondrion-related organelles (MROs). Depending on the completeness of the electron transport chain (ETC) and the organism's resulting type of energetic metabolism, as well as other retained and gained mitochondrial functions, MROs are traditionally classified into several categories: anaerobic mitochondria; hydrogen-producing mitochondria; hydrogenosomes; and mitosomes [2, 3]. However, it is now accepted that MROs exist in a functional and evolutionary continuum without sharp borders between categories [1, 4–7]. One extreme in this spectrum is the complete loss of the mitochondrion, as recently documented in the flagellate *Monocercomonoides* (Metamonada) [8]. Although comparative studies of highly reduced MRO forms are important for our understanding of the minimum requirements for cell function and energy production, they do not provide insight into the early stages of adaptation to anoxia [1].

Anaerobic lineages in the unicellular eukaryotic group Ciliophora (i.e., the ciliates) represent a unique opportunity to investigate the transition to, and evolution of, an anaerobic lifestyle, as the group contains numerous free-living and endobiotic lineages with varying levels of adaptation to anoxia, from microaerophiles to obligate anaerobes, as well as many occurrences of anaerobic species among otherwise aerobic lineages [9–13]. Although aerobic ciliates have been subjects of intensive research for centuries and include the important model organisms *Tetrahymena thermophila* [14] and *Paramecium tetraurelia* [15], their anaerobic relatives are notably understudied in comparison. Despite the advent of genomic approaches to the study of energetic metabolism in numerous anaerobic lineages across the tree of life

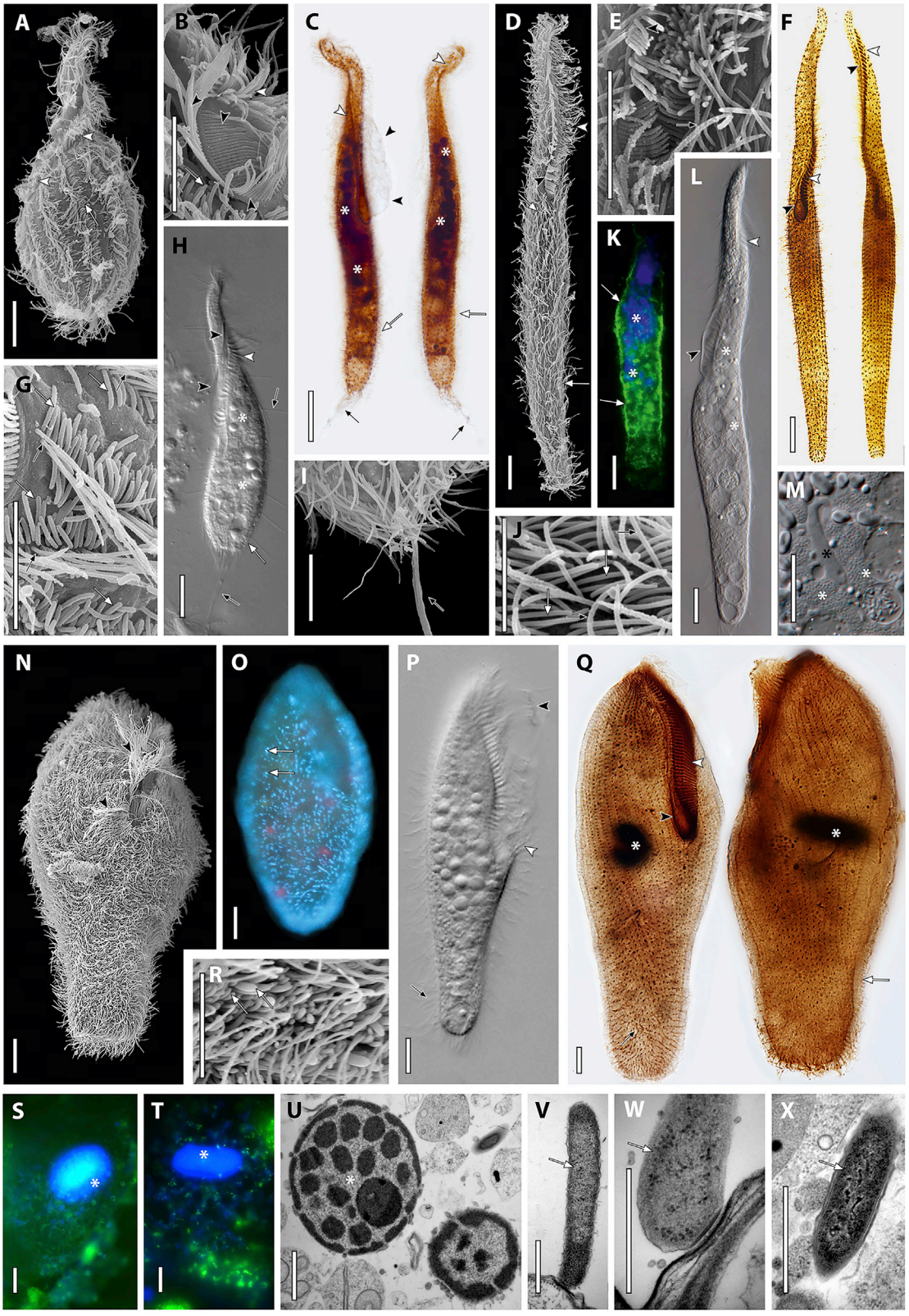

(legend on next page)

(e.g., metamonads, Archamoebae, breviates, Microsporidia, and Rhizaria) [1, 7, 8, 16], our knowledge of the metabolism of anaerobic ciliates has long been limited to the genome of a single species—the cockroach endobiont *Nyctotherus ovalis* (Armophorea) [17].

Similar to most endobiotic obligate anaerobes, such as the well-studied *Trichomonas*, *Giardia*, and *Entamoeba* [1], the MROs of armophorean ciliates, including that of *N. ovalis*, are known to produce hydrogen [18, 19]. However, the hydrogen-producing mitochondrion of *N. ovalis* retains its own genome and maintains a surprisingly complex metabolism [17, 18], closely resembling that of the human parasite *Blastocystis* (Stramenopiles) [20]. Nevertheless, studying the metabolism of an endobiont without an available comparison to its free-living relatives significantly obscures the complete image of the evolutionary adaptations to anoxic conditions, because it is difficult to distinguish adaptations associated with the transition to endobiosis from those associated with the adoption of an anaerobic lifestyle. Authors of a recent publication [21] have broadened the dataset with mitochondrial genomes and transcriptomes of four free-living anaerobic ciliates from the same class as the endobiotic *N. ovalis* (Armophorea), showing their common traits in encoding proton-pumping complex I but likely lacking functional complexes III and V of the ETC, therefore having lost the capacity for ATP synthesis via oxidative phosphorylation. *In silico* analyses indicate that all of them produce ATP by substrate-level phosphorylation via acetate:succinyl coenzyme A (CoA) transferase (ASCT) and succinyl-CoA synthetase (SCS).

Despite the fact that ciliates are known to thrive in anoxic environments [19], the number of independent origins of anaerobiosis in ciliates remains uncertain because of the absence of genomic data from many of them, preventing resolution of phylogenetic relationships in the phylum. Current data suggest at least four transitions to an anaerobiotic lifestyle in the major group titled CONThreeP [11, 22, 23], and at least several have likely occurred in another large group called SAL, which contains classes Spirotrichea, Armophorea, Litostomatea, and presumably also Odontostomatea and Cariacotrichea [11–13, 24]. Along with the obligately anaerobic Armophorea, Odontostomatea, and Cariacotrichea, the predominantly aerobic Litostomatea and Spirotrichea both include anaerobic taxa [10, 25].

Here, we present the discovery of two new classes of free-living anaerobic ciliates that host prokaryotic symbionts. Our comprehensive phylogenomic analysis reveals that these lineages, along with the class Armophorea, form a major clade of obligate anaerobes. To enhance our understanding of the evolution of anaerobiosis in ciliates, we used metagenomic and transcriptomic data to predict the mitochondrial metabolism within this clade. We predict functional adaptations present in their last common ancestor that likely led to the successful colonization and diversification of the group in various anoxic environments. We also employed transmission electron microscopy and fluorescence *in situ* hybridization microscopy to investigate their organelles and symbionts. Furthermore, we discuss the possible relationship of one of the two lineages to the uncultured deep-sea class Cariacotrichea. The data presented here provide new insights into the early stages of the transition to an obligately anaerobic lifestyle. On the basis of these findings, we propose evolutionary mechanisms underlying such changes, whereby association with the prokaryotic symbiont allows, and possibly constrains, its host to permanently reside in the anoxic environment by increasing host's metabolic efficiency via consuming hydrogen produced by the MROs, as previously confirmed in some anaerobic ciliates [19].

RESULTS AND DISCUSSION

Two Novel Ciliate Classes of Obligate Marine Anaerobes within the SAL Group

We isolated and cultured 13 strains (see Table S1) of anaerobic ciliates representing a novel, deep-branching lineage commonly inhabiting marine and brackish anoxic sediments. Our phylogenetic analyses of 18S rRNA and 28S rRNA genes, as well as phylogenomic analysis based on 124 protein-coding genes, show that this lineage branches within the SAL group but separately from all known classes, forming a strongly supported clade (Figures 2A and 2C). It comprises two morphologically distinct species (Figures 1 and S2; Tables S2 and S3;

Figure 1. Morphology and Ultrastructure of Muranotrichea and Parablepharismea Species and Their Symbionts

Morphology of *Muranothrix gubernata* gen. et sp. nov. (A–C and G–I), *Thigmothrix strigosa* gen. et sp. nov. (D–F and J–M), and *Parablepharisma* sp. (N–R), in life (H, L, M, and P), after protargol impregnation (C, F, and Q), in scanning electron microscope (SEM) (A, B, D, E, G, I, J, N, and R), and transmission electron microscope (TEM) (U–X).

(A, C, D, F, H, L, N, P, and Q) Left and right lateral views of a representative specimen.

(B) SEM detail of tripartite paroral membrane.

(E) SEM detail of bipartite paroral membrane.

(K, S, and T) CARD FISH showing (K and T) ectosymbiotic and free-living delta-proteobacterial bacteria (green), (S) archaea (green), and DAPI-stained macronuclei (blue).

(G, J, and R) SEM detail of ectosymbionts.

(I) SEM detail showing elongated cilia, emerging from tuft of short caudal cilia, used by *M. gubernata* as a rudder to speedily turn directions.

(M) Differential interference contrast (DIC) detail of J-shaped micronucleus (marked by black asterisk).

(O) Autofluorescence of F420 coenzyme showing ectosymbiotic methanogens (blue).

(R) SEM detail showing two morphotypes of ectosymbionts.

(U) TEM detail of nuclei.

(V, W, and X) TEM micrographs showing the connection of ectosymbionts (V and W) and an endosymbiont (X).

For more details on morphology and ultrastructure, see Figure S2. Morphological and ultrastructural features of selected strains of each species were studied in living cells, protargol-impregnated cells, and by scanning and transmission electron microscopy and are described in detail in taxonomic summary (Data S1) and Tables S1–S3. Black arrow, ciliature; white arrow, ectosymbiotic cells; black arrowhead, paroral membrane; white arrowhead, adoral zone of membranelles; white asterisk, macronuclei; black asterisk, micronucleus. Scale bars, (A–T) 10 μm and (U–X) 1 μm.

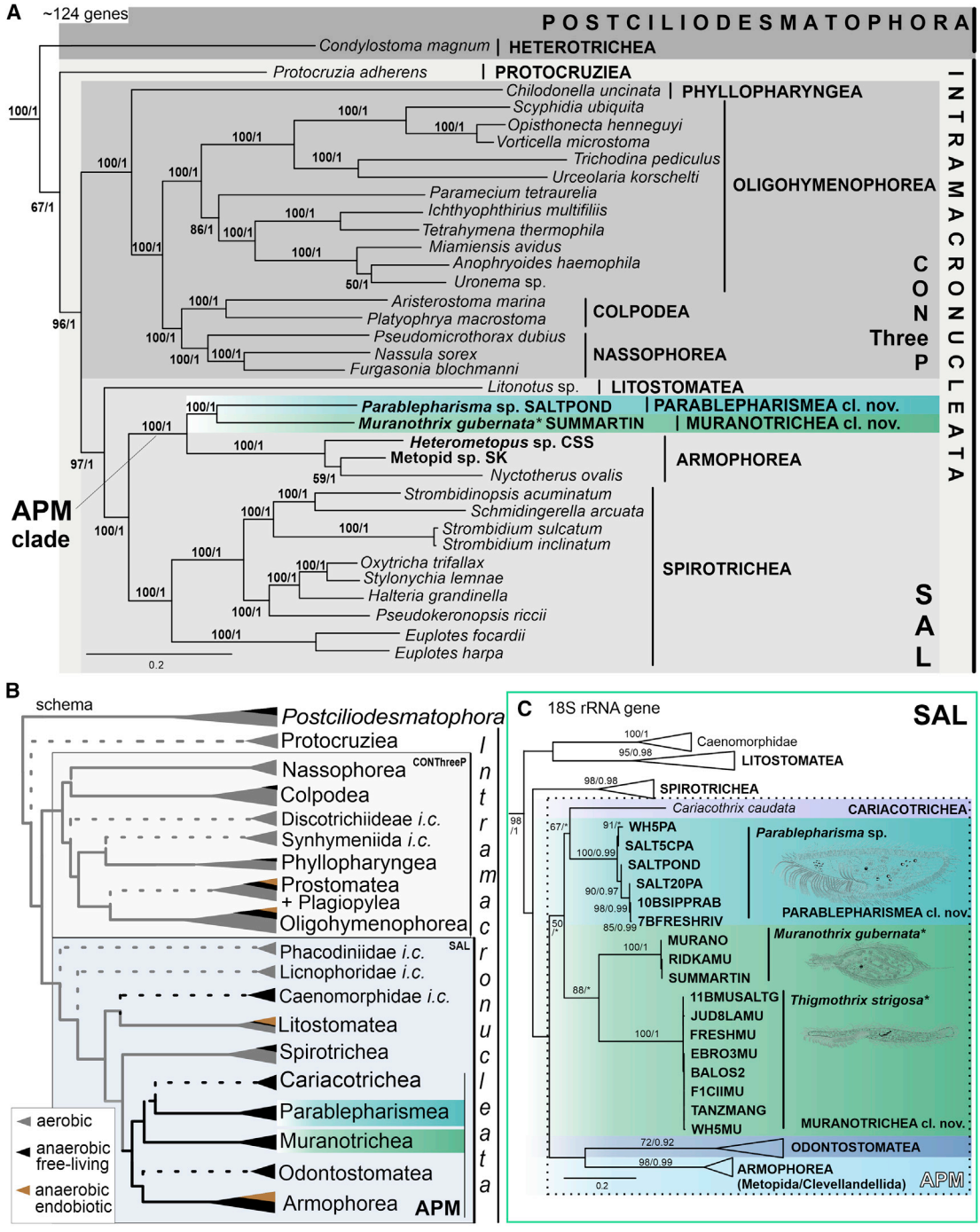

Figure 2. Phylogenetics of Ciliates with Emphasis on Anaerobic Ciliates in SAL Clade

(A) Phylogenomic tree of ciliates based on 124 gene sequences. The tree was constructed by the maximum likelihood method (GTRGAMMAI model) and is unrooted.

(B) Schema showing representation of anaerobes within Ciliophora.

(C) Inset of phylogenetic tree of ciliates from the SAL group based on the 18S rRNA gene sequences and inferred from the complete dataset (see full tree in Figure S1). The tree was constructed by the maximum likelihood method (GTRGAMMAI model) and is unrooted. The values at the branches represent statistical support in maximum likelihood bootstrap values/Bayesian posterior probabilities. Support values below 50/0.90 are not shown or are represented by an asterisk (*). An asterisk (*) in node tips marks gen. et sp. nov.

New sequences in bold with GenBank: MT177189–GenBank: MT177205 and GenBank: MT231936 (see Table S1 for further information about the sequenced strains).

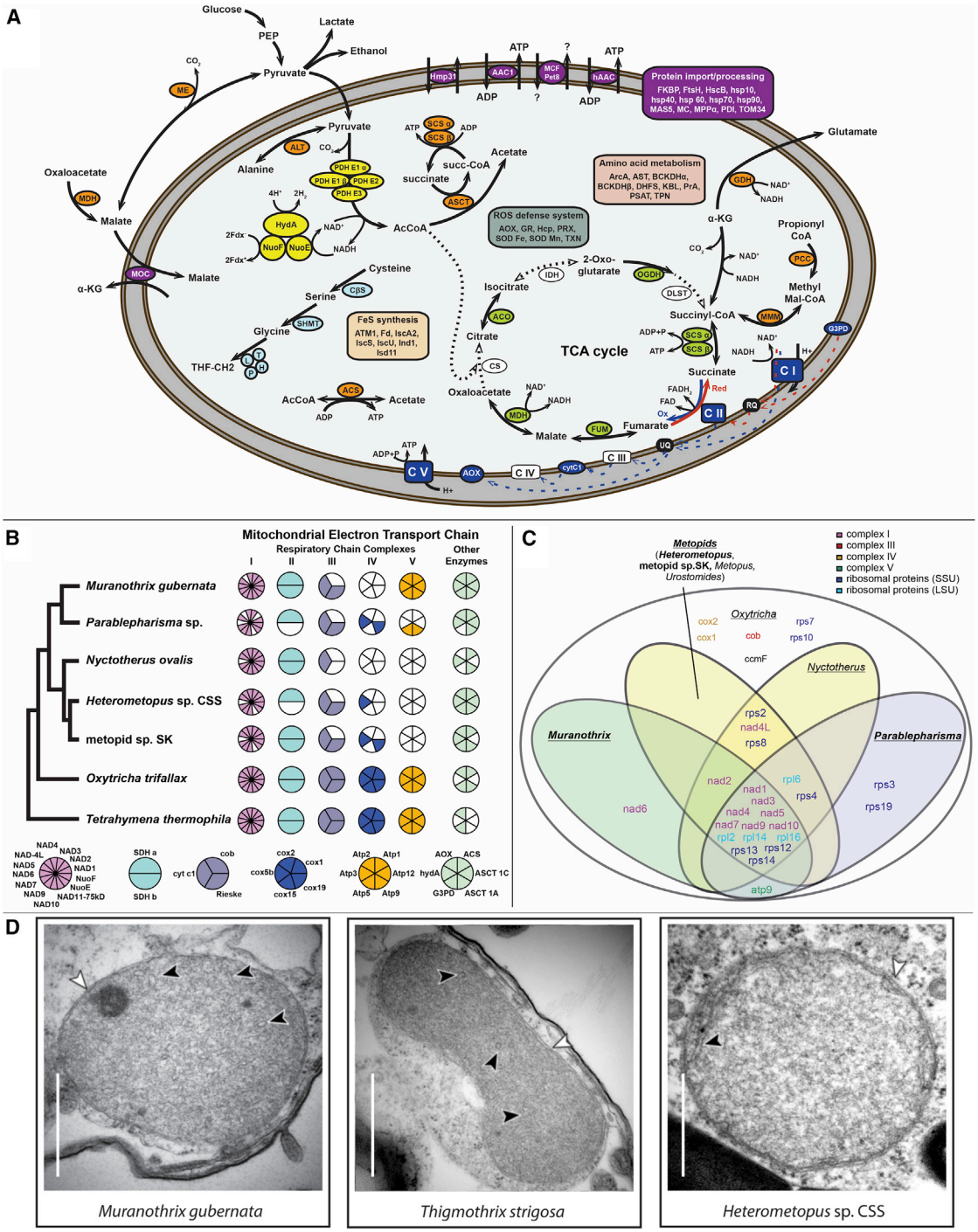

Figure 3. Mitochondrial Metabolism of APM Ciliates

(A) *In silico* prediction of the mitochondrial metabolism of the last shared ancestor of APM ciliates based on transcriptome and metagenome data generated in this study (for single gene trees, see Data S2). Full names for abbreviated proteins are included in Table S4. In dark blue are electron transport chain (ETC) complexes (see also B) and associated genes, purple are genes associated with transmembrane processes and protein import, green is the TCA cycle, yellow is pyruvate decarboxylation and [FeFe]-hydrogenase, light blue is glycine metabolism, orange is other enzymatic reactions, quinones are in black, UQ is ubiquinone and RD is rhodoquinone, proteins in white are absent, and white ETC complexes are missing proteins (see B) and presumed non-functional. Black dotted lines represent typical aerobic mitochondrial reactions presumed non-functional due to protein loss. Gray dashed lines represent predicted electron flow through the ETC when exposed to oxygen, and red dashed lines indicate anaerobic function for reduction of fumarate to succinate.

(B) Cartoon phylogenetic tree with Coulson plots representing presence and absence of ETC and other proteins important for mitochondrial metabolism from *Muranothrix gubernata*, *Parablepharisma* sp., *Nyctotherus ovalis* (from [17] and [21]), *Heterometopus* sp. CSS, metopid sp. SK, *Oxytricha trifallax* [34], and *Tetrahymena thermophila* [35].

(legend continued on next page)

Data S1), herein described as *Muranothrix gubernata*, gen. et sp. nov. and *Thigmothrix strigosa* gen. et sp. nov., which are classified within the newly established family Muranotrichidae, fam. nov. *Muranothrix gubernata* is recognizable by the elongated pear shape of the cell and leftward spiralization of somatic ciliary rows: by the presence of multiple macronuclei and single globular micronucleus, tripartite paroral membrane, a tuft of caudal cilia with a group of cohesive elongated cilia in the center, which it uses for rapid adjustment of locomotion direction (Figures 1A–1C and 1G–1I). In addition, it hosts typically arranged ectosymbionts (Figures 1G, 1V, and 1W). *Thigmothrix strigosa* differs by a slender cell shape lacking spiralization, J-shaped micronucleus, bipartite paroral membrane, absence of elongated caudal cilia, and presence of distinctly longer ectosymbionts (Figures 1D–1F and 1J–1M). Detailed information about the morphology, morphometric data, and taxonomic summary with diagnoses are shown in Supplemental Information. On the basis of the phylogenetic position and morphological distinctiveness of the two species in the family Muranotrichidae, we herein classify them as members of the new class Muranotrichea cl. nov.

In addition, we have isolated six strains of the genus *Parablepharisma* (Table S1), previously classified morphologically as a heterotrich belonging to the subphylum Postciliodesmatophora [26]. Although representatives of the genus *Parablepharisma* are commonly found in easily accessible shallow brackish and marine sediments and the genus itself was described nearly a century ago, it has not gained much attention since. Our phylogenomic analysis has shown that it is not only unrelated to Heterotrichea, but it is excluded from the Postciliodesmatophora and instead forms a deep lineage within the SAL group (subphylum Intramacronucleata) with a sister relationship to the herein described class, Muranotrichea (Figure 2A; Data S1). The exclusion of *Parablepharisma* from the Postciliodesmatophora is also supported morphologically by the absence of stacked postciliary microtubular ribbons to the right of somatic kineties (postciliodesmata). On the basis of its unique combination of morphological characteristics (Figures 1N–1T; see Table S3 and Data S1) and its phylogenetic placement within the SAL group, we describe this obligately anaerobic brackish lineage as Parablepharismea, cl. nov. comprising a single family, Parablepharismidae. These findings are further supported by a recent taxonomic study [27], providing an 18S rRNA gene sequence for two *Parablepharisma* species.

New Ciliate Classes and Uncultured, Deep-Ocean Cariacotrichea Likely Form a Clade

Our 124-gene phylogenomic analysis robustly resolved relationships among representatives of the SAL group with available genomic or transcriptomic data (Figure 2A). Muranotrichea and Parablepharismea form a clade branching sister to Armophorea ciliates (which are herein considered as Metopida+Clevelandellida, excluding Caenomorphidae that likely has a polyphyletic relationship with Metopida and Clevelandellida) [28, 29]. Together, the three lineages comprise a well-supported clade of obligate anaerobes, herein abbreviated as APM ciliates, which is sister to the predominantly aerobic Spirotrichea.

A confident interpretation of phylogenetic relationships among anaerobic ciliates is hampered by a paucity of genomic data. Therefore, we performed phylogenetic analysis of 18S rRNA gene sequences that includes data from other known obligate anaerobes within SAL (Odontostomatea, Caenomorphidae, and Cariacotrichea). This analysis, with broader taxon sampling, offers a notably different view on the evolution of anaerobiosis within ciliates (Figures 2B and S1); however, it was not sufficient to resolve most internal relationships within the SAL group and several relationships lacked support. The 18S rRNA gene tree placed Muranotrichea, Parablepharismea, Cariacotrichea, Odontostomatea, and Armophorea (Metopida+Clevelandellida without Caenomorphidae) in a clade where Cariacotrichea branches sister to Parablepharismea with moderate support. The sister relationship of Cariacotrichea to other species of *Parablepharisma* was also recovered by a recent study [27]. The inferred relationship of these lineages predicts the existence of a species-rich clade of morphologically diverse, marine obligate anaerobes.

The relationship between Parablepharismea and Cariacotrichea is of particular interest. Cariacotrichea includes enigmatic, uncultured deep-sea ciliates whose marker genes have been detected only a few times [12, 30], whereas the easily cultivable and cosmopolitan Parablepharismea inhabit saltmarshes and shallow brackish or marine sediments of the sublittoral zone (Table S1). Cultivation of species related to Cariacotrichea provides an opportunity to make inferences regarding the evolution of these obscure deep-sea ciliates. However, confirmation of their affinities necessitates genome-scale data from the anoxic zone-dwelling Cariacotrichea.

Mitochondrial Cristae Are Retained in Muranotrichea, Indicating Their Complex Mitochondrial Metabolism

Typical mitochondria possess invaginations in the inner mitochondrial membrane called cristae, which create a structure for the ETC complexes, but many MROs have completely lost their cristae as a part of their functional reduction [31]. Interestingly, some obligately anaerobic ciliates retain remnants of mitochondrial cristae, suggesting that their MRO metabolism is not as reduced as that of other obligate anaerobes. This has been observed in *Nyctotherus ovalis*, metopids (Armophorea) [18, 21, 32], and in Muranotrichea species described herein. Using transmission electron microscopy, we observed MROs with small inconspicuous vesiculations in *Muranothrix* (Figures 3D and S2) and more prominent invaginations of the inner membrane in *Thigmothrix* (Figures 3D and S2), which might represent cristae remnants. In contrast, the MROs of *Parablepharisma pellitum*, as shown in the micrographs of Fenchel and Finlay [19, 33], are dense structures with no visible cristae; however, further confirmation is needed. Anaerobic ciliates might have retained cristae despite the successful transition to obligate anaerobiosis

(C) Venn diagram showing presence of genes retained on organellar genomes of *M. gubernata*, *Parablepharisma* sp., *N. ovalis* [21], Metopida, and *O. trifallax* [34]. Remark: *Urostomides* [36] represents *Metopus striatus*, as used in [21].

(D) Transmission electron microscopy micrographs showing mitochondrion-related organelles of studied ciliates—*M. gubernata*, *T. strigosa*, and *Heterometopus* sp. CSS. Black arrowhead, vesiculations; white arrowhead, double membrane. Scale bars, 400 nm.

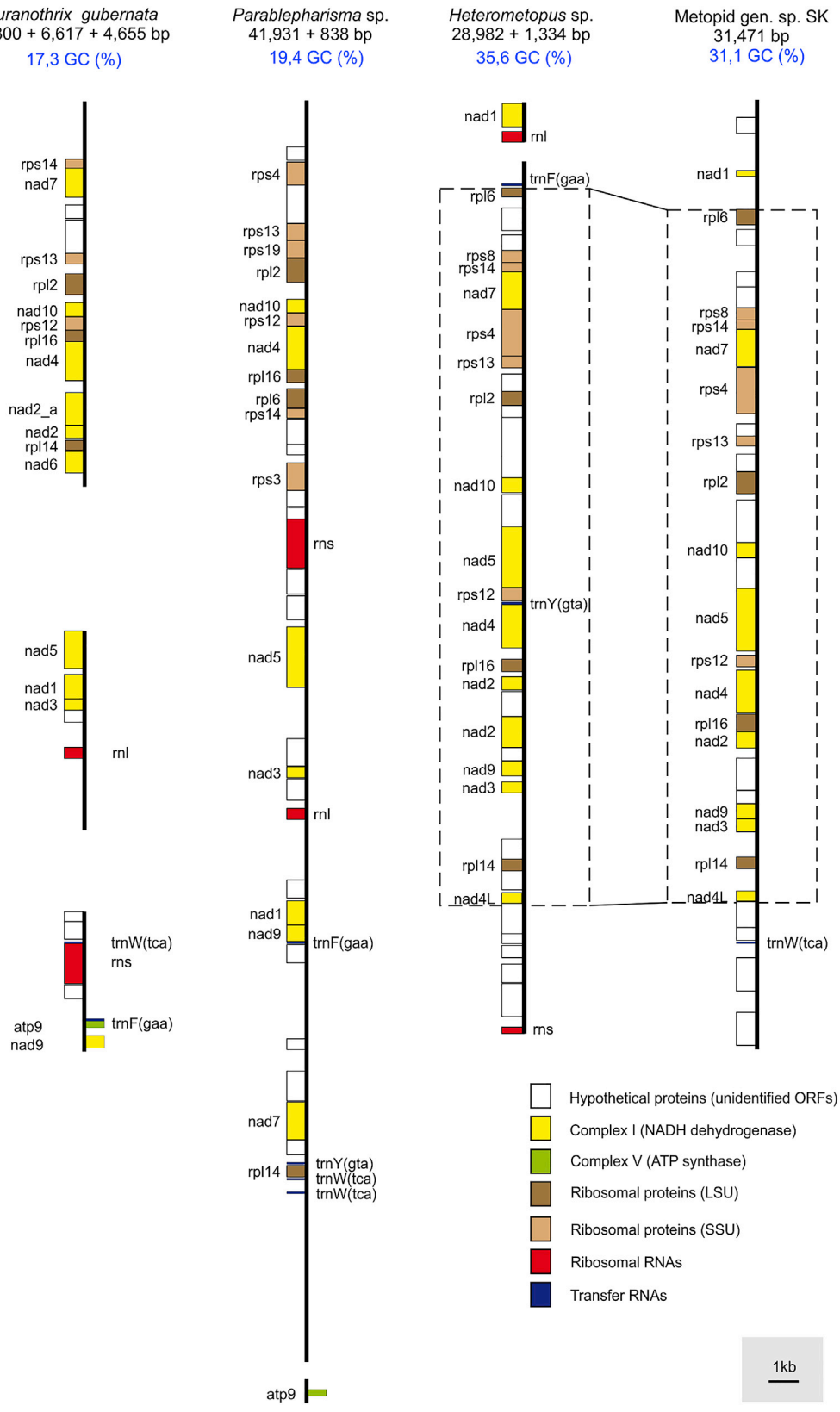

(legend on next page)

to serve as functional space for remaining ETC enzymes, such as complex V [31].

Energetic Metabolism of Anaerobic Ciliates with Emphasis on Armophorea, Parablepharismea, and Muranotrichea

To characterize the metabolic capacity of anaerobic ciliates across the APM clade (Armophorea-Parablepharismea-Muranotrichea), we sequenced metagenomes from metopid sp. SK (Armophorea), *Heterometopus* sp. CSS (Armophorea), and *Parablepharisma* sp. SALTPOND (Parablepharismea), along with both metagenome and transcriptome from *Muranothrix gubernata* SUMMARTIN (Muranotrichea). Estimates of assembly completeness, based on presence or absence of 124 genes in phylogenomic analyses, are as follows: *Muranothrix gubernata* 67%; *Parablepharisma* sp. 68%; *Heterometopus* sp. CSS 81%; and metopid sp. SK 84%. In combination with data published for four ciliates belonging to the Armophorea [17, 21], we used the APM clade of ciliates to explore nuances in a continuum of reductive evolution resulting from the adaptation to anaerobiosis. Members of all three classes possess signatures of classical mitochondrial pathways, including amino acid metabolism, fatty acid metabolism, and Fe-S cluster biogenesis (see Table S4). Furthermore, all three classes retain mitochondrial genomes (Figures 3C and 4), which encode genes for ribosomal subunits and subunits of some ETC complexes. On the basis of the total genetic makeup of APM ciliates, we have reconstructed the predicted mitochondrial metabolism of the last common ancestor of APM, which appears to have been adapted to hypoxic conditions (Figure 3A).

Patterns of Reductive Evolution in the ETC

In a canonical aerobic mitochondrion, the ETC is a series of enzymatic complexes that transfer electrons and protons along a membrane with oxygen serving as the terminal electron acceptor. The generated proton gradient is ultimately used by complex V (F_1F_O-ATP synthase) to produce ATP. Modifications, including complete loss of the ETC, have been observed in anaerobic taxa across the tree of life [1, 6, 8]. We found complex I and II to be nearly complete in all four ciliates investigated in this study (Figure 3B), consistent with the retention of ETC complex I and II genes observed in other anaerobic ciliate taxa [17, 21] and suggesting that they remain functional for recycling NAD+ and FAD+ throughout APM ciliates. Furthermore, we identified two complex III subunits, Rieske protein and cytochrome *c*1, in all four studied species, indicating the presence of a more complete complex III in the ancestor of APM ciliates. On the other hand, the absence of the cytochrome b (*cob*) gene in all species strongly suggests that complex III is not functional. We also identified the complex IV proteins, cytochrome *c* oxidase subunit 5b (cox5b) and cytochrome *c* oxidase assembly factor (cox19), in the metagenome data from Armophorea and Parablepharismea; however, the absence of any complex IV proteins in the *Muranothrix* transcriptome and the published *Nyctotherus* transcriptome and expressed sequence tag (EST) data [17, 21] indicates the complex IV is non-functional or completely missing from these taxa. There is a possibility that the Rieske protein and cytochrome *c*1 from complex III and cox5b and cox19 from complex IV are retained for alternative yet unknown functions.

Proteins comprising subunits of complex V are missing entirely from all Armophorea species investigated to date [17, 18, 21], including those published in this study. Surprisingly, we found a complete complex V in *Muranothrix* and both macronuclear gamma subunit of ATP synthase (atp3) and mitochondrial ATP synthase subunit 9 (atp9) in *Parablepharisma*. On the basis of this, we believe that *Muranothrix* is unique among APM ciliates in its likely capability of generating ATP by using the proton gradient generated by complex I. The retention of *atp9* gene in the *Parablepharisma* mitochondrion genome suggests it might also retain a functional complex V that we were unable to identify because of the fragmented dataset. The identification of genes from all five complexes of the ETC, including complete complexes I, II, and V, in some representatives, indicates the last common ancestor of APM ciliates was likely a facultative or obligate anaerobe capable of using a proton gradient generated by complex I as a proton pump for the production of ATP by complex V.

Interpretations of the links between reductive ETC evolution and NADH-generating metabolism in MROs provide insights to the principles of mitochondrial adaptations to anaerobiosis. Complex I and II likely remain under selection as they are both involved in recycling NAD+ and FAD+, which are essential for other organellar processes. Interestingly, the APM ciliates also possess [FeFe]-hydrogenase fused with NuoE and NuoF NADH dehydrogenases, providing them with another path to recycle NAD+ (see below). This suggests that, in most of the APM lineages, complex I is utilized primarily to generate and maintain the proton gradient for other organelle functions than ATP synthesis. Without complex V, an excess proton gradient generated by fully functioning complex I might be detrimental for the cell because of reactive oxygen species creation. Loss of genes from complexes III and IV is observed in diverse anaerobes [1], and these complexes are typically downregulated in hypoxic conditions even in mammalian cells [37, 38]. A full transition to anaerobiosis leads to reduced selective pressure and eventual loss of these genes.

Rhodoquinone Biosynthesis

In aerobic conditions, complex II oxidizes succinate to fumarate, thereby transferring electrons for the reduction of ubiquinone to ubiquinol, although in anaerobic conditions, complex II functions in reverse. The lower redox potential of rhodoquinone over ubiquinone enables rhodoquinone to transfer electrons via complex II, reducing fumarate to succinate [39]. Methyltransferase *rqu*A was demonstrated to directly convert ubiquinone to rhodoquinone [40] and has been acquired by some anaerobic protists through at least two independent lateral gene transfer (LGT) events [41]. Although rhodoquinone has been detected in *Nyctotherus* [18], *rqu*A has not been found in any APM ciliate investigated to date, including those in this study [17, 21, 42]. Using an *rqu*A hidden Markov model, we identified several other methyltransferase-like genes that are shared among APM ciliates, but

Figure 4. Mitochondrial Genomes Obtained in This Study

Graphical maps of partial mitochondrial genomes obtained in this study. Corresponding sequences are deposited in DRYAD: https://doi.org/10.5061/dryad.vx0k6djnm. The two metopid genomes reveal high level of synteny as indicated by dashed lines.

no *rqu*A homolog was identified (data not shown). Considering that rhodoquinone has been detected in *N. ovalis* [18], we suspect that a yet unidentified methyltransferase-like gene is responsible for the conversion of ubiquinone to rhodoquinone in APM ciliates.

The TCA Cycle Is Not Functional in Anaerobic Ciliates

With the loss of a functional complex III and complex IV, MROs regenerate quinone by using electrons from rhodoquinol when reducing fumarate to succinate. This negates a need for a functional tricarboxylic acid (TCA) cycle as observed in most hydrogenosomes, where the TCA cycle is functionally incomplete, and all TCA proteins that do remain function in other pathways. We observed the same pattern in APM ciliates, where we found evidence for malate dehydrogenase, aconitase, and 2-oxogluterate dehydrogenase (pyruvate dehydrogenase [PDH] E3). Other TCA cycle proteins, including citrate synthase and isocitrate dehydrogenase, are absent from all APM ciliates that have been investigated to date [17, 21].

[FeFe]-Hydrogenase Conserved among Diverse Anaerobic Ciliates

Typical hydrogenosomes, such as those described from trichomonads, possess a monomeric Fe-hydrogenase enzyme and its requisite maturases (HydE, HydF, and HydG) [1, 43]. These are not found in the APM ciliates described here and elsewhere [17, 18, 21]; however, all APM ciliates investigated to date encode a trimeric [FeFe]-hydrogenase that is fused with the 24 kD and 51 kD subunits of a bacterial complex I, forming a heterotrimeric enzyme [17, 18, 21, 44]. The same formation of the heterotrimeric [FeFe]-hydrogenase was described from the anaerobic hydrogen-producing bacterium, *Thermotoga maritima*, and was classified as an electron bifurcating enzyme capable of driving oxidation of NADH to H_2 through the use of both NADH and reduced ferredoxin as simultaneous electron donors [45]. This [FeFe]-hydrogenase is unique among eukaryotes, and the electron bifurcation enables anaerobic ciliates to produce H_2 and convert NADH to NAD in what would otherwise be a thermodynamically unfavorable reaction [45].

In its initial discovery, the [FeFe]-hydrogenase was recognized as unusual among eukaryotes and likely of a different evolutionary origin [18, 44]. In a subsequent study, the [FeFe]-hydrogenase was recognized as the only LGT that conclusively encoded an enzyme localized to the mitochondrion in *Nyctotherus* [17]. Homologs of this [FeFe]-hydrogenase were recently identified in two anaerobic ciliates outside SAL clade—*Plagiopyla* (Plagiopylea) and *Cyclidium* (Oligohymenophorea)—and proposed its ancestral gain pre-adapting ciliates for early transitions to oxygen-depleted environments [21]. The [FeFe]-hydrogenase sequences identified in our data from metopid SK, *Heterometopus*, *Parablepharisma*, and *Muranothrix* branch together with such sequences from *Nyctotherus* and *Metopus* [17, 21] within a fully supported ciliate clade (Data S2), compliant with the ancestral acquisition of this gene in ciliates [21]. However, to elucidate its origin, its further investigation among various aerobic and anaerobic ciliates is needed.

Pyruvate Metabolism

Diverse anaerobic eukaryotes utilize pyruvate:ferredoxin oxidoreductase (PFO) to convert pyruvate to acetyl CoA. Instead of PFO, we find all four subunits of the typical PDH in metopid sp. SK, and partial PDH from *Heterometopus* and *Muranothrix*. A complete PDH complex was also found in *N. ovalis* and *M. contortus* [17, 21], indicating that a functional PDH was present in the ancestor of APM ciliates; however, we were unable to detect any PDH subunits in *Parablepharisma*. The absence of PDH is more likely the result of an incomplete metagenomic dataset rather than a loss of PDH in *Parablepharisma*. The presence of malate dehydrogenase in all ciliates investigated here and identification of malic enzyme in *Parablepharisma*, *Heterometopus*, and metopid sp. SK indicates that pyruvate is being imported via the malate aspartate shuttle in APM ciliates. The identification of ASCT homologs and SCS in *N. ovalis* and *M. contortus* [17, 21] suggests that ciliate MROs can also produce ATP from acetyl CoA by substrate-level phosphorylation. We found two homologs of ASCT in all three classes of anaerobic ciliates in this study, and SCS subunits were also recognized in Armophorea and Muranotrichea. Our findings, along with the identification of ASCT and SCS in *Plagiopyla frontata* and *Cyclidium porcatum* [21], support generation of ATP by substrate-level phosphorylation as a core feature of ciliate hydrogen-producing mitochondria.

Muranotrichea and Parablepharismea Harbor Consortia of Distinct Prokaryotic Symbionts

In addition to their ability to penetrate a broad range of environments, ciliates are also known for a tendency to form various symbiotic relationships, whether as hosts or symbionts themselves [46]. In point of fact, representatives from all the above-discussed lineages of previously described anaerobic ciliates host various prokaryotic symbionts [12, 19, 28, 33] that utilize hydrogen produced by the MROs of their hosts to form methane or hydrogen sulfide via processes of methanogenesis and sulfate reduction, respectively [19, 47, 48]. Congruently, all three species of Muranotrichea and Parablepharismea from this study are hosts to rod-shaped symbionts showing different morphologies and orientations in each species (Figures 1G, 1J, 1R, and 1U–1W). Although the short, plump ectosymbionts of *Muranothrix* (Figures 1A and 1G) attach end on along ciliary rows and thinner ectosymbionts of *Thigmothrix* (Figures 1D and 1J) lie parallel to the host cortex (Figures S2A and S2C), a thick coat of perpendicularly attached, elongated rods of several morphotypes carpets the entire surface of *Parablepharisma* (Figures 1N, 1R, and S2L). We applied probes specific to sulfate-reducing delta-proteobacteria by using a sensitive method of catalyzed reporter deposition fluorescence *in situ* hybridization (CARD FISH) to *T. strigosa* and *Parablepharisma* sp. and obtained a positive signal localized on the outside of the cells (Figure 1K), and there was a more thinly distributed signal in *Parablepharisma* (Figure 1T). Surprisingly, in *Parablepharisma*, we also obtained a strong cortical autofluorescence signal for F_{420} coenzyme (Figure 1O), typical for some methanogens (and, rarely, other prokaryotes, such as Actinobacteria) [49], suggesting the identity of the second symbiont morphotype, further supported by CARD FISH with Archaea-specific probes (Figure 1S). To our knowledge, ectosymbiotic methanogens have never before been recorded in free-living protists, being known only from rumen ciliates [50]. They were not detected in Muranotrichea, which host non-methanogenic endosymbionts (Figure 1X). The ectosymbionts of *Parablepharisma pellitum* were shown to be inserted in pits in the cell membrane, and MROs were closely

attached on the cytosolic side [19, 33], suggesting that they utilize hydrogen produced by the host's MROs. This hypothesis is supported by the finding of the [FeFe]-hydrogenase in all APM ciliates whose genomes have been studied to date [21] as well as hydrogen production levels measured in Armophorea [19]. Ectosymbionts of both Muranotrichea species are often attached to the host (Figures 1V and 1W), where MROs are localized close to the cell surface (Figures S2E and S2F), although the endobionts do not seem to be in tight association with the MROs, though sometimes located nearby (Figure 1X).

More often than not, symbiotic relationships do not represent an exclusive, stable mutualism but a dynamic and competitive interaction for resources between several players, as shown in the scuticociliate sp. GW7 (Oligohymenophorea) [51]. On the other hand, two anaerobic symbiotic groups hosted by *Parduczia* sp. (Karyorelictea) seemingly cycle H_2 alone without any contribution of the ciliate [52, 53] but providing a refuge, where the symbiotic prokaryotes interact protected from the outside world of predation and competition [19, 54]. Moreover, these unique "niches" likely alter local biogeochemistry [52, 53], accenting the often overlooked role of these symbioses in our ecosystems.

Symbiosis-Associated Evolutionary Mechanism of Transitions to Obligate Anaerobiosis

As previously described, adaptations to an anaerobic lifestyle are associated with changes in morphology and metabolic capabilities of the mitochondrion [21, 31, 55]. The predicted mitochondrial metabolism of representatives from the APM ciliates reveals functional adaptations and subsequent modifications of metabolic pathways that were present in their last common ancestor and likely led to the successful colonization and diversification of the group in various anoxic environments, including marine, freshwater, and endobiotic gut habitats. The prevalence of anaerobic lifestyle in ciliates and particularly in the SAL group is striking (see Figure 2B), leading us to the most basic of questions—why?

Transitions to anaerobic lifestyles in free-living eukaryotes have likely developed under the influence of multiple factors. It is thought that decreased predation risk and reduced resource competition experienced in anoxic habitats are likely to be strong ecological factors that drive organisms to expand into these niches [56]. Aerobic ciliates are known to commonly migrate into anoxic zones and feed on anaerobic bacteria [19, 57–59]. Some are able to survive the temporary anoxia possibly thanks to the oxygen produced by their prey plastids or intracellular photosymbionts (e.g., green algae *Chlorella*), capable of oxygenic photosynthesis in low-light conditions [57, 58, 60]. Furthermore, ciliates might have had metabolic pre-adaptations facilitating their proclivity to penetrate oxygen-depleted environments—heterotrimeric [FeFe]-hydrogenase, present in unrelated ciliate lineages and possibly acquired early in the evolution of ciliates [21], potentially allows the ciliate to maintain cellular redox balance in anoxia by oxidizing NADH and regenerating NAD+ for glycolysis [21], as it does in numerous anaerobic bacteria [45]. Regardless of the prior events, what has led the presumably facultative anaerobe to turn to anoxia permanently and lose the ability to return?

Eukaryotic-prokaryotic partnerships appear crucial to ciliate adaptation to anoxia [47, 61]. Although experiments have demonstrated that some anaerobic ciliates can survive when depleted of their symbionts [19], to our knowledge, no symbiont-free anaerobic representative of the SAL group has been found in nature. In environments with scarce resources or strong competition, consorting with the right type of symbiotic partners might provide the crucial fitness advantage for exploiting a new niche and can lead to novel adaptation, diversification, and speciation. We propose a scenario where metabolic byproducts of the host (such as hydrogen or acetate) attracted anaerobic prokaryotes and led to their association with the ciliate cell. For the host, an advantage of maintaining prokaryotic symbionts is the faster removal of undesirable hydrogen and other metabolic waste, such as acetate, from the cell, improving the rate and efficiency of the host's energetic metabolism, as confirmed, besides anaerobic ciliates, also in breviates [19, 62]. Both Muranotrichea and Parablepharismea, like some other anaerobic ciliates [51, 52], host multiple symbionts that might not only interact with their hosts but also among themselves. Competition for hydrogen molecules and other metabolic byproducts likely further increases the rate of hydrogen removal from the host cells and improves the efficiency of the host's energetic metabolism.

We hypothesize that the increased energy yield enabled by symbionts, in turn, allowed these ciliate lineages to persist in extended periods of residency in anoxia. Over evolutionary time, prolonged periods in anoxic habitats might have driven the loss of aerobic metabolic functions because of relaxed selection on these traits [63], leading ultimately to obligate anaerobiosis. Although we cannot deduce the identity of partners in symbioses established prior to, or early in, the transition to obligate anaerobiosis in ciliates, we can hypothesize as to the mechanisms underlying establishment of the symbioses and benefits of maintaining the relationship for both partners. Sulfate-reducing bacteria might have been attracted by the metabolic waste release from the ciliate cell and subsequently attached to the ciliate, eventually becoming permanent ectosymbionts. Environmental methanogenic archaea were undoubtedly consumed by the ciliate and occasionally escaped digestion. Maintenance of functional methanogens alive within the cell, in the direct proximity of MROs, allowing them to utilize the mitochondrial metabolic waste, such as hydrogen or acetate, would have been more advantageous for host cell than energy yielded by their digestion. The consequent boost of host's metabolic rate might be particularly important for ciliates, because over two-thirds of metabolic energy produced by their aerobic respiration was indicated as used solely for motility [64].

Because the majority of APM lineages inhabit marine sediments and the clade possibly includes the ectosymbiont-bearing deep-sea Cariacotrichea [12], we can assume that their last common ancestor might also have been a marine ciliate. After the species radiation, ciliates likely have changed their symbionts because of multiple transitions into freshwater and endobiotic habitats. However, establishing independent novel symbioses might have been a simpler process because of host cell adaptations to these interactions, potentially including losses in genes for aerobic metabolism, hindering a return to aerobic environments. Considering the estimated number of anaerobiosis origins in ciliates, their species richness, colonization of diverse environments, and broad spectrum of symbionts, it is not surprising to find varying levels and directions of the

evolution in these relationships. In some cases, such as the methanogen symbiont in marine *Metopus contortus*, the interaction might lead to a reduction of the symbiont genome, suggesting an early transition to obligate endosymbiosis [65]. In others, like the freshwater *Heterometopus* sp. CSS, the prokaryote might remain relatively independent, keeping its genome largely intact [66]. Although this might reflect a younger evolutionary age of the relationship, it might also suggest that hosts could eventually lose its symbiont and replace it with another to maintain the advantages without deeper investments [67]. On the other hand, such a contrast could represent distinct pathways of adaptation to anoxia in marine versus freshwater environment, where predation, competition, and sources of energy vary.

Ciliates have adapted to an anaerobic lifestyle repeatedly across numerous independent lineages (Figure 2B), making them an ideal model for comparing patterns of reductive evolution of mitochondrial metabolism in response to adaptation to low-oxygen environments. Most deep lineages in the ciliate super-group SAL are anaerobic, as only Spirotrichea and Litostomatea contain aerobic species. If we infer the last common ancestor of SAL lineages to be aerobic species, at least three independent transitions to anaerobic lifestyle must have occurred, that is, all lineages in SAL for which genomic data are available—Spirotrichea, Litostomatea, and the APM clade formed by Armophorea, Muranotrichea, and Parablepharismea. However, if we consider also taxa without available genomic data, we discover at least one more possible anaerobiosis origin in Caenomorphidae (Armophorida, possibly sister to Litostomatea) [28, 29] and discrete species among both prevalently aerobic Spirotrichea and Litostomatea [59, 68, 69]. Furthermore, single-gene analyses suggest that two more anaerobic lineages, the deep-sea Cariacotrichea and Odontostomatea, are members of the APM clade as well, which further affirms that the last common ancestor of APM clade was likely an anaerobe and its evolution leads to radiation of five deep distinct lineages of anaerobic ciliates that inhabit various anoxic environments.

Although ciliates are known to demand higher levels of energy because of their large cell size and fast movement [64], many are apparently capable of producing sufficient levels of ATP in low levels of oxygen. The prediction of energetic metabolism in APM ciliates shows that substrate-level phosphorylation alone can supply cells with sufficient ATP, without significantly limiting energetically demanding functions. Thus, we confirm that a canonical mitochondrion is not necessary for sustaining large and highly complex eukaryotic cells with a large genome size [70]. This is in contrast with the small cell size of the majority of other anaerobic protists, which have often undergone high levels of reduction of their mitochondria, frequently lost mitochondrial genomes, and sometimes even completely lost the mitochondrion, as documented in the small-sized *Monocercomonoides*, which produces energy entirely via extended glycolysis pathway and fermentation [8]. To our knowledge, no data confirming symbionts in *Monocercomonoides* are available.

We argue that symbiotic anaerobic prokaryotes play a crucial role in driving a transition to an obligately anaerobic lifestyle via removing excess byproducts from its host's cell and enabling faster metabolism rate, ultimately leading to loss of the functional aerobic metabolism while maintaining the high energy production levels necessary for large and active cells. However, such symbiotic relationships are not known only from ciliates but also from some other anaerobic protists, for example, Archamoebae (Amoebozoa), Psalteriomonadidae (Heterolobosea), or Anaeramoebidae (Eukaryota *incertae sedis*) [71–73], for which energy demands are not known, and thus, it is necessary to obtain such data from more anaerobic protists to confirm whether this hypothesis is generally plausible. In addition, methanogenic archaea and sulfate-reducing bacteria are by no means the only hydrogen-utilizing symbionts of anaerobic protists, as shown in small marine species *Lenisia limosa* (Breviatea), where its symbiont *Arcobacter* (Campylobacterota) oxidizes hydrogen produced by the host's MROs, congruently increasing the ATP yield [62]. We predict that future research into other microbial symbioses in anoxic environments will provide solid evidence about the role of symbionts in the transition to obligatory anaerobiosis.

STAR★METHODS

Detailed methods are provided in the online version of this paper and include the following:

- KEY RESOURCES TABLE
- RESOURCE AVAILABILITY
  - Lead Contact and Materials Availability
  - Data and Code Availability
- EXPERIMENTAL MODEL AND SUBJECT DETAILS
  - Formal Treatment of New Taxa and Taxonomic Summary
  - Biological Samples and Cultivation of Organisms
  - Cell Processing and Fixation
- METHOD DETAILS
  - Light and Electron Microscopy
  - Fluorescence Microscopy and CARD-FISH
  - DNA/RNA Extraction, Amplification, and Library Preparations
  - Sanger Sequencing and Illumina NextSeq Sequencing
  - Metagenomic and Transcriptomic Assemblies
  - Datasets preparation and rRNA gene phylogenetic analyses
  - Phylogenomic analyses
  - In-silico predictions of mitochondrial metabolism
- QUANTIFICATION AND STATISTICAL ANALYSIS

SUPPLEMENTAL INFORMATION

Supplemental Information can be found online at https://doi.org/10.1016/j.cub.2020.03.064.

ACKNOWLEDGMENTS

The authors are grateful to the anonymous reviewers for their constructive comments. Thank you also belongs to Tereza Gebouská, Vilém Helešic, Lucie Juřičková, Jan Pyrih, Anna Schrecengost, and František Šťáhlavský for collecting numerous samples; to Miroslav Hyliš from Charles University for kindly assisting with the scanning microscopy procedures; and to Štěpán Kosík for Latin and Greek language supervision. The work was supported by the Grant Agency of the Czech Republic (project 19-19297S) and Charles University specific research grant SVV 260571/2020, providing funding for I.Č., J.R., and M.K. J.R. was also supported by Grant Agency of Charles University (project 251234). E.S. was supported by International Mobilities of Researchers of

the Biology Centre CZ.02.2.69/0.0/0.0/16_027/0008357. R.A.B. was supported by National Science Foundation OCE-PRF 1322928. M.K. was supported by Fellowship Purkynė (Czech Acad. Sci.) and by the ERD fund "Centre for Research of Pathogenicity and Virulence of Parasites" (CZ.02.1.01/0.0/0.0/16_019/0000759). T.P. has been supported by Charles University Research Centre program number 204069. An acknowledgment belongs to MetaCentrum VO (https://metavo.metacentrum.cz/en/), which was used for conducing *de novo* assembly of Illumina reads.

AUTHOR CONTRIBUTIONS

I.Č. and J.R. isolated studied taxa and maintained isolates in long-term cultures. I.Č., V.P.E., R.A.B., and J.R. have designed the experimental work and research strategy. I.Č., V.P.E., R.A.B., and M.K. have secured the execution of sequencing procedures. R.A.B. and J.R. obtained and processed DNA and RNA for metagenomes and transcriptome sequencing, respectively. R.A.B., V.P.E., M.K., and J.R. conducted analyses of both metagenomic and transcriptomic sequence data. I.Č., M.K., D.Ž., and J.R. performed phylogenetic and phylogenomic analyses. E.S., M.K., P.T., T.P., and J.R. performed analysis of mitochondrial metabolism. W.B. and J.R. performed morphological and ultrastructural studies and described novel taxa. J.R. led writing of the manuscript. All authors interpreted the results and contributed to the manuscript preparation.

DECLARATION OF INTERESTS

The authors declare no competing interests.

Received: February 1, 2020
Revised: March 10, 2020
Accepted: March 24, 2020
Published: April 23, 2020

REFERENCES

1. Stairs, C.W., Leger, M.M., and Roger, A.J. (2015). Diversity and origins of anaerobic metabolism in mitochondria and related organelles. Philos. Trans. R. Soc. Lond. B Biol. Sci. *370*, 20140326.
2. Embley, T.M., and Martin, W. (1998). A hydrogen-producing mitochondrion. Nature *396*, 517–519.
3. Müller, M., Mentel, M., van Hellemond, J.J., Henze, K., Woehle, C., Gould, S.B., Yu, R.-Y., van der Giezen, M., Tielens, A.G.M., and Martin, W.F. (2012). Biochemistry and evolution of anaerobic energy metabolism in eukaryotes. Microbiol. Mol. Biol. Rev. *76*, 444–495.
4. Stairs, C.W., Eme, L., Brown, M.W., Mutsaers, C., Susko, E., Dellaire, G., Soanes, D.M., van der Giezen, M., and Roger, A.J. (2014). A SUF Fe-S cluster biogenesis system in the mitochondrion-related organelles of the anaerobic protist Pygsuia. Curr. Biol. *24*, 1176–1186.
5. Maguire, F., and Richards, T.A. (2014). Organelle evolution: a mosaic of 'mitochondrial' functions. Curr. Biol. *24*, R518–R520.
6. Gawryluk, R.M.R., Kamikawa, R., Stairs, C.W., Silberman, J.D., Brown, M.W., and Roger, A.J. (2016). The earliest stages of mitochondrial adaptation to low oxygen revealed in a novel Rhizarian. Curr. Biol. *26*, 2729–2738.
7. Leger, M.M., Kolísko, M., Kamikawa, R., Stairs, C.W., Kume, K., Čepička, I., Silberman, J.D., Andersson, J.O., Xu, F., Yabuki, A., et al. (2017). Organelles that illuminate the origins of *Trichomonas* hydrogenosomes and *Giardia* mitosomes. Nat. Ecol. Evol. *1*, 0092.
8. Karnkowska, A., Vacek, V., Zubáčová, Z., Treitli, S.C., Petrželková, R., Eme, L., Novák, L., Žárský, V., Barlow, L.D., Herman, E.K., et al. (2016). A eukaryote without a mitochondrial organelle. Curr. Biol. *26*, 1274–1284.
9. Fenchel, T., Perry, T., and Thane, A. (1977). Anaerobiosis and symbiosis with bacteria in free-living ciliates. J. Protozool. *24*, 154–163.
10. Embley, T.M., Finlay, B.J., Dyal, P.L., Hirt, R.P., Wilkinson, M., and Williams, A.G. (1995). Multiple origins of anaerobic ciliates with hydrogenosomes within the radiation of aerobic ciliates. Proc. Biol. Sci. *262*, 87–93.
11. Lynn, D.H. (2008). The Ciliated Protozoa: Characterization, Classification, and Guide to the Literature, Third Edition (Springer Science & Business Media).
12. Orsi, W., Edgcomb, V., Faria, J., Foissner, W., Fowle, W.H., Hohmann, T., Suarez, P., Taylor, C., Taylor, G.T., Vd'acný, P., et al. (2012). Class Cariacotrichea, a novel ciliate taxon from the anoxic Cariaco Basin, Venezuela. Int. J. Syst. Evol. Microbiol. *62*, 1425–1433.
13. Fernandes, N.M., Vizzoni, V.F., Borges, B.D.N., Soares, C.A.G., da Silva-Neto, I.D., and Paiva, T.D.S. (2018). Molecular phylogeny and comparative morphology indicate that odontostomatids (Alveolata, Ciliophora) form a distinct class-level taxon related to Armophorea. Mol. Phylogenet. Evol. *126*, 382–389.
14. Ruehle, M.D., Orias, E., and Pearson, C.G. (2016). Tetrahymena as a unicellular model eukaryote: Genetic and genomic tools. Genetics *203*, 649–665.
15. Beisson, J., Bétermier, M., Bré, M.H., Cohen, J., Duharcourt, S., Duret, L., Kung, C., Malinsky, S., Meyer, E., Preer, Jr., J.R., et al. (2010). *Paramecium tetraurelia*: the renaissance of an early unicellular model. Cold Spring Harb. Protoc. *2010*, pdb-emo140.
16. Nývltová, E., Stairs, C.W., Hrdý, I., Rídl, J., Mach, J., Pačes, J., Roger, A.J., and Tachezy, J. (2015). Lateral gene transfer and gene duplication played a key role in the evolution of Mastigamoeba balamuthi hydrogenosomes. Mol. Biol. Evol. *32*, 1039–1055.
17. de Graaf, R.M., Ricard, G., van Alen, T.A., Duarte, I., Dutilh, B.E., Burgtorf, C., Kuiper, J.W.P., van der Staay, G.W.M., Tielens, A.G.M., Huynen, M.A., and Hackstein, J.H. (2011). The organellar genome and metabolic potential of the hydrogen-producing mitochondrion of Nyctotherus ovalis. Mol. Biol. Evol. *28*, 2379–2391.
18. Boxma, B., de Graaf, R.M., van der Staay, G.W.M., van Alen, T.A., Ricard, G., Gabaldón, T., van Hoek, A.H.A.M., Moon-van der Staay, S.Y., Koopman, W.J.H., van Hellemond, J.J., et al. (2005). An anaerobic mitochondrion that produces hydrogen. Nature *434*, 74–79.
19. Fenchel, T., and Finlay, B.J. (1991). The biology of free-living anaerobic ciliates. Eur. J. Protistol. *26*, 201–215.
20. Stechmann, A., Hamblin, K., Pérez-Brocal, V., Gaston, D., Richmond, G.S.S., van der Giezen, M., Clark, C.G., and Roger, A.J. (2008). Organelles in Blastocystis that blur the distinction between mitochondria and hydrogenosomes. Curr. Biol. *18*, 580–585.
21. Lewis, W.H., Lind, A.E., Sendra, K.M., Onsbring, H., Williams, T.A., Esteban, G.F., Hirt, R.P., Ettema, T.J.G., and Embley, T.M. (2020). Convergent evolution of hydrogenosomes from mitochondria by gene transfer and loss. Mol. Biol. Evol. *37*, 524–539.
22. Gentekaki, E., Kolísko, M., Boscaro, V., Bright, K.J., Dini, F., Di Giuseppe, G., Gong, Y., Miceli, C., Modeo, L., Molestina, R.E., et al. (2014). Large-scale phylogenomic analysis reveals the phylogenetic position of the problematic taxon Protocruzia and unravels the deep phylogenetic affinities of the ciliate lineages. Mol. Phylogenet. Evol. *78*, 36–42.
23. Foissner, W., and Foissner, I. (1995). Fine structure and systematic position of Enchelyomorpha vermicularis (Smith, 1899) Kahl, 1930, an anaerobic ciliate (Protozoa, Ciliophora) from domestic sewage. Acta Protozool. *34*, 21–34.
24. Gentekaki, E., Kolísko, M., Gong, Y., and Lynn, D. (2017). Phylogenomics solves a long-standing evolutionary puzzle in the ciliate world: The subclass Peritrichia is monophyletic. Mol. Phylogenet. Evol. *106*, 1–5.
25. Boscaro, V., Syberg-Olsen, M.J., Irwin, N.A.T., Del Campo, J., and Keeling, P.J. (2019). What can environmental sequences tell us about the distribution of low-rank taxa? The case of Euplotes (Ciliophora, Spirotrichea), including a description of Euplotes enigma sp. nov. J. Eukaryot. Microbiol. *66*, 281–293.
26. Kahl, A. (1932). Urtiere oder Protozoa I: Wimpertiere oder Ciliata (Infusoria) 3. Spirotricha. Tierwelt Dtl *25*, 399–650.
27. Campello-Nunes, P.H., Fernandes, N.M., Szokoli, F., Fokin, S.I., Serra, V., Modeo, L., Petroni, G., Soares, C.A.G., da S. Paiva, T., and da Silva-Neto, I.D. (2020). *Parablepharisma* (Ciliophora) is not a heterotrich: a

phylogenetic and morphological study with the proposal of new taxa. Protist *171*, 125716.

28. Rotterová, J., Bourland, W., and Čepička, I. (2018). Tropidoatractidae fam. nov., a deep branching lineage of Metopida (Armophorea, Ciliophora) found in diverse habitats and possessing prokaryotic symbionts. Protist *169*, 362–405.
29. Li, S., Bourland, W.A., Al-Farraj, S.A., Li, L., and Hu, X. (2017). Description of two species of caenomorphid ciliates (Ciliophora, Armophorea): morphology and molecular phylogeny. Eur. J. Protistol. *61*, 29–40..
30. Edgcomb, V., Orsi, W., Taylor, G.T., Vdacny, P., Taylor, C., Suarez, P., and Epstein, S. (2011). Accessing marine protists from the anoxic Cariaco Basin. ISME J. *5*, 1237–1241.
31. Muñoz-Gómez, S.A., Slamovits, C.H., Dacks, J.B., Baier, K.A., Spencer, K.D., and Wideman, J.G. (2015). Ancient homology of the mitochondrial contact site and cristae organizing system points to an endosymbiotic origin of mitochondrial cristae. Curr. Biol. *25*, 1489–1495.
32. Akhmanova, A., Voncken, F., van Alen, T., van Hoek, A., Boxma, B., Vogels, G., Veenhuis, M., and Hackstein, J.H.P. (1998). A hydrogenosome with a genome. Nature *396*, 527–528.
33. Fenchel, T., and Finlay, B.J. (1995). Ecology and Evolution in Anoxic Worlds (Oxford University).
34. Swart, E.C., Bracht, J.R., Magrini, V., Minx, P., Chen, X., Zhou, Y., Khurana, J.S., Goldman, A.D., Nowacki, M., Schotanus, K., et al. (2013). The Oxytricha trifallax macronuclear genome: a complex eukaryotic genome with 16,000 tiny chromosomes. PLoS Biol. *11*, e1001473.
35. Smith, D.G.S., Gawryluk, R.M.R., Spencer, D.F., Pearlman, R.E., Siu, K.W.M., and Gray, M.W. (2007). Exploring the mitochondrial proteome of the ciliate protozoon Tetrahymena thermophila: direct analysis by tandem mass spectrometry. J. Mol. Biol. *374*, 837–863.
36. Bourland, W., Rotterová, J., and Čepička, I. (2017). Morphologic and molecular characterization of seven species of the remarkably diverse and widely distributed metopid genus Urostomides Jankowski, 1964 (Armophorea, Ciliophora). Eur. J. Protistol. *61* (Pt A), 194–232.
37. Vijayasarathy, C., Damle, S., Prabu, S.K., Otto, C.M., and Avadhani, N.G. (2003). Adaptive changes in the expression of nuclear and mitochondrial encoded subunits of cytochrome c oxidase and the catalytic activity during hypoxia. Eur. J. Biochem. *270*, 871–879.
38. Fukuda, R., Zhang, H., Kim, J.W., Shimoda, L., Dang, C.V., and Semenza, G.L.L. (2007). HIF-1 regulates cytochrome oxidase subunits to optimize efficiency of respiration in hypoxic cells. Cell *129*, 111–122.
39. Tielens, A.G.M., Rotte, C., van Hellemond, J.J., and Martin, W. (2002). Mitochondria as we don't know them. Trends Biochem. Sci. *27*, 564–572.
40. Bernert, A.C., Jacobs, E.J., Reinl, S.R., Choi, C.C.Y., Roberts Buceta, P.M., Culver, J.C., Goodspeed, C.R., Bradley, M.C., Clarke, C.F., Basset, G.J., and Shepherd, J.N. (2019). Recombinant RquA catalyzes the in vivo conversion of ubiquinone to rhodoquinone in Escherichia coli and Saccharomyces cerevisiae. Biochim. Biophys. Acta Mol. Cell Biol. Lipids *1864*, 1226–1234.
41. Stairs, C.W., Eme, L., Muñoz-Gómez, S.A., Cohen, A., Dellaire, G., Shepherd, J.N., Fawcett, J.P., and Roger, A.J. (2018). Microbial eukaryotes have adapted to hypoxia by horizontal acquisitions of a gene involved in rhodoquinone biosynthesis. eLife *7*, e34292.
42. Yan, Y., Maurer-Alcalá, X.X., Knight, R., Kosakovsky Pond, S.L., and Katz, L.A. (2019). Single-cell transcriptomics reveal a correlation between genome architecture and gene family evolution in ciliates. MBio *10*, 1–13.
43. Pütz, S., Doležal, P., Gelius-Dietrich, G., Boháčová, L., Tachezy, J., and Henze, K. (2006). Fe-hydrogenase maturases in the hydrogenosomes of Trichomonas vaginalis. Eukaryot. Cell *5*, 579–586.
44. Boxma, B., Ricard, G., van Hoek, A.H.A.M., Severing, E., Moon-van der Staay, S.Y., van der Staay, G.W.M., van Alen, T.A., de Graaf, R.M., Cremers, G., Kwantes, M., et al. (2007). The [FeFe] hydrogenase of Nyctotherus ovalis has a chimeric origin. BMC Evol. Biol. *7*, 230.
45. Schut, G.J., and Adams, M.W.W. (2009). The iron-hydrogenase of Thermotoga maritima utilizes ferredoxin and NADH synergistically: a new perspective on anaerobic hydrogen production. J. Bacteriol. *191*, 4451–4457.
46. Dziallas, C., Allgaier, M., Monaghan, M.T., and Grossart, H.P. (2012). Act together-implications of symbioses in aquatic ciliates. Front. Microbiol. *3*, 288.
47. Hackstein, J.H.P. (2010). Anaerobic ciliates and their methanogenic endosymbionts. In (Endo)symbiotic Methanogenic Archaea, J.H.P. Hackstein, ed. (Springer), pp. 13–24.
48. Fenchel, T., and Ramsing, N.B. (1992). Identification of sulphate-reducing ectosymbiotic bacteria from anaerobic ciliates using 16S rRNA binding oligonucleotide probes. Arch. Microbiol. *158*, 394–397.
49. Greening, C., Ahmed, F.H., Mohamed, A.E., Lee, B.M., Pandey, G., Warden, A.C., Scott, C., Oakeshott, J.G., Taylor, M.C., and Jackson, C.J. (2016). Physiology, biochemistry, and applications of F420- and Fo-dependent redox reactions. Microbiol. Mol. Biol. Rev. *80*, 451–493.
50. Vogels, G.D., Hoppe, W.F., and Stumm, C.K. (1980). Association of methanogenic bacteria with rumen ciliates. Appl. Environ. Microbiol. *40*, 608–612.
51. Takeshita, K., Yamada, T., Kawahara, Y., Narihiro, T., Ito, M., Kamagata, Y., and Shinzato, N. (2019). Tripartite symbiosis of an anaerobic scuticociliate with two hydrogenosome-associated endosymbionts, a *Holospora*-related alphaproteobacterium and a methanogenic archaeon. Appl. Environ. Microbiol. *85*, e00854-19.
52. Beinart, R.A., Beaudoin, D.J., Bernhard, J.M., and Edgcomb, V.P. (2018). Insights into the metabolic functioning of a multipartner ciliate symbiosis from oxygen-depleted sediments. Mol. Ecol. *27*, 1794–1807.
53. Fenchel, T. (1993). Methanogenesis in marine shallow water sediments: The quantitative role of anaerobic protozoa with endosymbiotic methanogenic bacteria. Ophelia *37*, 67–82.
54. Beinart, R.A. (2019). The significance of microbial symbionts in ecosystem processes. mSystems *4*, 1–5.
55. Embley, T.M., van der Giezen, M., Horner, D.S., Dyal, P.L., Bell, S., and Foster, P.G. (2003). Hydrogenosomes, mitochondria and early eukaryotic evolution. IUBMB Life *55*, 387–395.
56. Paulmier, A., and Ruiz-Pino, D. (2009). Oxygen minimum zones (OMZs) in the modern ocean. Prog. Oceanogr. *80*, 113–128.
57. Finlay, B.J., Maberly, S.C., and Esteban, G.F. (1996). Spectacular abundance of ciliates in anoxic pond water: contribution of symbiont photosynthesis to host respiratory oxygen requirements. FEMS Microbiol. Ecol. *20*, 229–235.
58. Esteban, G.F., Finlay, B.J., and Clarke, K.J. (2009). Sequestered organelles sustain aerobic microbial life in anoxic environments. Environ. Microbiol. *11*, 544–550.
59. Bernard, C., and Fenchel, T. (1996). Some microaerobic ciliates are facultative anaerobes. Eur. J. Protistol. *32*, 293–297.
60. Sørensen, M.E.S., Wood, A.J., Minter, E.J.A., Lowe, C.D., Cameron, D.D., and Brockhurst, M.A. (2020). Comparison of independent evolutionary origins reveals both convergence and divergence in the metabolic mechanisms of symbiosis. Curr. Biol. *30*, 328–334.e4.
61. Edgcomb, V.P., Leadbetter, E.R., Bourland, W., Beaudoin, D., and Bernhard, J.M. (2011). Structured multiple endosymbiosis of bacteria and archaea in a ciliate from marine sulfidic sediments: a survival mechanism in low oxygen, sulfidic sediments? Front. Microbiol. *2*, 55.
62. Hamann, E., Gruber-Vodicka, H., Kleiner, M., Tegetmeyer, H.E., Riedel, D., Littmann, S., Chen, J., Milucka, J., Viehweger, B., Becker, K.W., et al. (2016). Environmental Breviatea harbour mutualistic Arcobacter epibionts. Nature *534*, 254–258.
63. Lahti, D.C., Johnson, N.A., Ajie, B.C., Otto, S.P., Hendry, A.P., Blumstein, D.T., Coss, R.G., Donohue, K., and Foster, S.A. (2009). Relaxed selection in the wild. Trends Ecol. Evol. *24*, 487–496.
64. Katsu-Kimura, Y., Nakaya, F., Baba, S.A., and Mogami, Y. (2009). Substantial energy expenditure for locomotion in ciliates verified by means of simultaneous measurement of oxygen consumption rate and swimming speed. J. Exp. Biol. *212*, 1819–1824.

65. Lind, A.E., Lewis, W.H., Spang, A., Guy, L., Embley, T.M., and Ettema, T.J.G. (2018). Genomes of two archaeal endosymbionts show convergent adaptations to an intracellular lifestyle. ISME J. *12*, 2655–2667.
66. Beinart, R.A., Rotterová, J., Čepička, I., Gast, R.J., and Edgcomb, V.P. (2018). The genome of an endosymbiotic methanogen is very similar to those of its free-living relatives. Environ. Microbiol. *20*, 2538–2551.
67. Husník, F., and Keeling, P.J. (2019). The fate of obligate endosymbionts: reduction, integration, or extinction. Curr. Opin. Genet. Dev. *58-59*, 1–8.
68. Boscaro, V., Husník, F., Vannini, C., and Keeling, P.J. (2019). Symbionts of the ciliate Euplotes: diversity, patterns and potential as models for bacteria-eukaryote endosymbioses. Proc. Biol. Sci. *286*, 20190693.
69. Bernard, C., and Fenchel, T. (1994). Chemosensory behaviour of *Strombidium purpureum*, an anaerobic oligotrich with endosymbiotic purple non-sulphur bacteria. J. Eukaryot. Microbiol. *41*, 391–396.
70. Hampl, V., Čepička, I., and Eliáš, M. (2019). Was the mitochondrion necessary to start eukaryogenesis? Trends Microbiol. *27*, 96–104.
71. Broers, C.A.M., Meijers, H.H.M., Symens, J.C., Stumm, C.K., Vogels, G.D., and Brugerolle, G. (1993). Symbiotic association of Psalteriomonas vulgaris n. spec. with Methanobacterium formicicum. Eur. J. Protistol. *29*, 98–105.
72. Gutiérrez, G., Chistyakova, L.V., Villalobo, E., Kostygov, A.Y., and Frolov, A.O. (2017). Identification of Pelomyxa palustris Endosymbionts. Protist *168*, 408–424.
73. Táborský, P., Pánek, T., and Čepička, I. (2017). Anaeramoebidae fam. nov., a novel lineage of anaerobic amoebae and amoeboflagellates of uncertain phylogenetic position. Protist *168*, 495–526.
74. Lynn, D.H., Kolísko, M., and Bourland, W. (2018). Phylogenomic analysis of Nassula variabilis n. sp., Furgasonia blochmanni, and Pseudomicrothorax dubius confirms a nassophorean clade. Protist *169*, 180–189.
75. Stahl, D.A., and Amann, R. (1991). Development and application of nucleic acid probes in bacterial systematics. In Nucleic Acid Techniques in Bacterial Systematics, E. Stackebrandt, and M. Goodfellow, eds. (Wiley), pp. 205–248.
76. Lücker, S., Steger, D., Kjeldsen, K.U., MacGregor, B.J., Wagner, M., and Loy, A. (2007). Improved 16S rRNA-targeted probe set for analysis of sulfate-reducing bacteria by fluorescence in situ hybridization. J. Microbiol. Methods *69*, 523–528.
77. Medlin, L., Elwood, H.J., Stickel, S., and Sogin, M.L. (1988). The characterization of enzymatically amplified eukaryotic 16S-like rRNA-coding regions. Gene *71*, 491–499.
78. Bolger, A.M., Lohse, M., and Usadel, B. (2014). Trimmomatic: a flexible trimmer for Illumina sequence data. Bioinformatics *30*, 2114–2120.
79. Greiner, S., Lehwark, P., and Bock, R. (2019). OrganellarGenomeDRAW (OGDRAW) version 1.3.1: expanded toolkit for the graphical visualization of organellar genomes. Nucleic Acids Res. *47* (W1), W59–W64.
80. Hall, T.A. (1999). BIOEDIT: a user-friendly biological sequence alignment editor and analysis program for Windows 95/98/NT. Nucleic Acids Symp. Ser. *41*, 95–98.
81. Stamatakis, A. (2014). RAxML version 8: a tool for phylogenetic analysis and post-analysis of large phylogenies. Bioinformatics *30*, 1312–1313.
82. Nguyen, L.T., Schmidt, H.A., von Haeseler, A., and Minh, B.Q. (2015). IQ-TREE: a fast and effective stochastic algorithm for estimating maximum-likelihood phylogenies. Mol. Biol. Evol. *32*, 268–274.
83. Wang, H.C., Minh, B.Q., Susko, E., and Roger, A.J. (2018). Modeling site heterogeneity with posterior mean site frequency profiles accelerates accurate phylogenomic estimation. Syst. Biol. *67*, 216–235.
84. Lartillot, N., Lepage, T., and Blanquart, S. (2009). PhyloBayes 3: a Bayesian software package for phylogenetic reconstruction and molecular dating. Bioinformatics *25*, 2286–2288.
85. Katoh, K., and Standley, D.M. (2013). MAFFT multiple sequence alignment software version 7: improvements in performance and usability. Mol. Biol. Evol. *30*, 772–780.
86. Criscuolo, A., and Gribaldo, S. (2010). BMGE (block mapping and gathering with entropy): a new software for selection of phylogenetic informative regions from multiple sequence alignments. BMC Evol. Biol. *10*, 210.
87. Pasulka, A.L., Levin, L.A., Steele, J.A., Case, D.H., Landry, M.R., and Orphan, V.J. (2016). Microbial eukaryotic distributions and diversity patterns in a deep-sea methane seep ecosystem. Environ. Microbiol. *18*, 3022–3043.
88. Doddema, H.J., and Vogels, G.D. (1978). Improved identification of methanogenic bacteria by fluorescence microscopy. Appl. Environ. Microbiol. *36*, 752–754.
89. Foissner, W. (2014). An update of 'basic light and scanning electron microscopic methods for taxonomic studies of ciliated protozoa'. Int. J. Syst. Evol. Microbiol. *64*, 271–292.
90. Pernthaler, A., Pernthaler, J., and Amann, R. (2002). Fluorescence in situ hybridization and catalyzed reporter deposition for the identification of marine bacteria. Appl. Environ. Microbiol. *68*, 3094–3101.
91. Peng, Y., Leung, H.C.M., Yiu, S.M., and Chin, F.Y.L. (2012). IDBA-UD: a de novo assembler for single-cell and metagenomic sequencing data with highly uneven depth. Bioinformatics *28*, 1420–1428.
92. Alneberg, J., Bjarnason, B.S., de Bruijn, I., Schirmer, M., Quick, J., Ijaz, U.Z., Lahti, L., Loman, N.J., Andersson, A.F., and Quince, C. (2014). Binning metagenomic contigs by coverage and composition. Nat. Methods *11*, 1144–1146.
93. Eren, A.M., Esen, O.C., Quince, C., Vineis, J.H., Morrison, H.G., Sogin, M.L., and Delmont, T.O. (2015). Anvi'o: an advanced analysis and visualization platform for 'omics data. PeerJ *3*, e1319.
94. Parks, D.H., Imelfort, M., Skennerton, C.T., Hugenholtz, P., and Tyson, G.W. (2015). CheckM: assessing the quality of microbial genomes recovered from isolates, single cells, and metagenomes. Genome Res. *25*, 1043–1055.
95. Grabherr, M.G., Haas, B.J., Yassour, M., Levin, J.Z., Thompson, D.A., Amit, I., Adiconis, X., Fan, L., Raychowdhury, R., Zeng, Q., et al. (2011). Full-length transcriptome assembly from RNA-seq data without a reference genome. Nat. Biotechnol. *29*, 644–652.
96. Maddison, W.P., and Maddison, D.R. (2008). Mesquite: a modular system for evolutionary analysis. Version 3.04. http//mesquiteproject.org.
97. Fu, L., Niu, B., Zhu, Z., Wu, S., and Li, W. (2012). CD-HIT: accelerated for clustering the next-generation sequencing data. Bioinformatics *28*, 3150–3152.

STAR★METHODS

KEY RESOURCES TABLE

REAGENT or RESOURCE	SOURCE	IDENTIFIER
Biological Samples		
isolated ciliates	This study (Table S1)	GenBank: BioSample IDs SAMN07273875, SAMN07273876, SAMN07273879, SAMN14342334
Chemicals, Peptides, and Recombinant Proteins		
Citifluor	Citifluor Ltd.	Cat#AF1-25
Vectashield	Vector Laboratories	Cat#H-1200
10 mg/mL Lysozyme	Sigma – Aldrich	Cat#l3790
40 mg/mL Dextran Sulfate	Sigma – Aldrich	Cat#9011-18-1
0.4% Roche Blocking Reagent	Sigma – Aldrich	Cat#11096176001
pGEM-T Easy Vector System I	Promega	Cat#A1360
DNA/RNAShield	Zymo Research	Cat#R1100-50
TriReagent	Sigma – Aldrich	Cat#93289
DNase	QIAGEN	Cat#15200-50
Dynabeads Oligo(dT) 25 system	Thermo Fisher Scientific	Cat#61002
Proteinase K	Thermo Fisher Scientific	Cat#EO0491
Critical Commercial Assays		
Genomic DNA Kit II TM	Zymo Research	Cat#D3020
Genomic DNA Minikit	Geneaid	Cat#GB300
DNeasy Blood & Tissue Kit	QIAGEN	Cat#69506
RiboMinus kit	Thermo Fisher Scientific	Cat#A1083708
RNeasy Mini Kit	QIAGEN	Cat#74104
Deposited Data		
Permanent type specimen slides deposited in the collection of the National Museum in Prague, Czech Republic	This study (Data S1)	Inventory numbers P6E5001 – P6E5004
Raw sequence reads for both transcriptome and metagenomes generated in this study have been deposited to NCBI's GenBank under two unifying BioProject IDs.	This study	GenBank: PRJNA391713 and PRJNA614527
Metagenome assembly of *Heterometopus* sp. CSS deposited in GenBank	[66]	GenBank: GCA_003202625.1
Mitochondrial genomes deposited in Dryad	This study	Dryad: https://doi.org/10.5061/dryad.vx0k6djnm
Single gene datasets used for phylogenomic analysis deposited in Dryad	This study	Dryad: https://doi.org/10.5061/dryad.vx0k6djnm
Protein datasets used for mitochondrial pathway mapping deposited in Dryad	This study	Dryad: https://doi.org/10.5061/dryad.vx0k6djnm
18S rRNA gene sequences deposited in GenBank	This study	GenBank: MT177189, MT177190, MT177191, MT177192, MT177193, MT177194, MT177195, MT177196, MT177197, MT177198, MT177199, MT177200, MT177201, MT177202, MT177203, MT177204, MT177205, and MT231936
18S rRNA gene sequences of representative ciliates retrieved from GenBank, used as reference dataset	GenBank	https://www.ncbi.nlm.nih.gov/genbank
reference dataset for phylogenomic analyses	[24]	10.1016/j.ympev.2016.09.016
reference dataset for phylogenomic analyses	[74]	10.1016/j.protis.2018.02.002

(*Continued on next page*)

Continued

REAGENT or RESOURCE	SOURCE	IDENTIFIER
Genes of interests collected from previously published studies of anaerobic mitochondria	[4]	10.1098/rstb.2014.0326
Genes of interests collected from previously published studies of anaerobic mitochondria	[6]	10.1016/j.cub.2016.08.025
Genes of interests collected from previously published studies	[7]	10.1038/s41559-017-0092
Genes of interests collected from previously published studies	[17]	10.1093/molbev/msr059
Genes of interests collected from previously published studies	[18]	10.1186/1471-2148-7-230
Genes of interests collected from previously published studies	[35]	10.1016/j.jmb.2007.09.051
Experimental Models: Cell Lines		
JM109 competent cells of *Escherichia coli*	Promega	Cat#L2005; RRID: Addgene_49761
Oligonucleotides		
ARC915 (CTTGTCTCAGTCTCCG)	[75]	Not applicable
DELTA495a (AGTTAGCCGGCTTCCT), b(AGTTAGCCGGCTTCCT), c(AATTAGCCGGCTTCCT)	[76]	10.1016/j.mimet.2007.02.009
competitor DELTA495a (AGTTAGCCGGCTTCTT), b(AGTTAGCCGGCTTCKT), c(AATTAGCCGGCTTCTT)	[76]	10.1016/j.mimet.2007.02.009
MedlinA (5′-AACCTGGT TGATCCTGCCAGT-3′)	[77]	10.1016/0378-1119(88)90066-2
MedlinB (5′-GATCCTTCT GCAGGTTCACCTAC-3′)	[77]	10.1016/0378-1119(88)90066-2
Recombinant DNA		
pGEM-T Easy Vector System I	Promega	Cat#A1360
Softwares and Algorithms		
Quick Photo	Promicra, Czech Republic	https://www.promicra.com/
Rcorrector	https://github.com/mourisl/Rcorrector	https://doi.org/10.1186/s13742-015-0089-y
Trimmomatic	[78]	http://www.usadellab.org/cms/?page=trimmomatic
metaSPAdes	http://cab.spbu.ru/software/spades/	https://doi.org/10.1007/978-3-642-37195-0_13
MFannot	https://megasun.bch.umontreal.ca/cgibin/dev_mfa/mfannotInterface.pl	http://megasun.bch.umontreal.ca/RNAweasel/
OGDRAW	[79]	https://chlorobox.mpimp-golm.mpg.de/OGDraw.html
BLAST	[80]	https://blast.ncbi.nlm.nih.gov/
RAxML	[81]	https://sco.hits.org/exelixis/web/software/raxml/
IQ TREE	[82]	http://www.iqtree.org/
PMSF	[83]	http://www.iqtree.org/
Phylobayes	[84]	http://www.atgc-montpellier.fr/phylobayes/
MAFFT	[85]	https://mafft.cbrc.jp/alignment/software/
BMGE	[86]	ftp://ftp.pasteur.fr/pub/gensoft/projects/BMGE/
trimal	[87]	http://trimal.cgenomics.org/

(*Continued on next page*)

Continued

REAGENT or RESOURCE	SOURCE	IDENTIFIER
Barrel-O-Monkeys	http://rogerlab.biochemistryandmolecularbiology.dal.ca/monkeybarrel.php	Not applicable
Raw_prediction.py	https://github.com/DavidZihala/raw_gene_prediction	Not applicable

RESOURCE AVAILABILITY

Lead Contact and Materials Availability

Further information and requests for resources should be directed to and will be fulfilled by the Lead Contact, Johana Rotterová (johana.rotterova@natur.cuni.cz). This study did not generate new unique reagents.

Data and Code Availability

Metagenomic and transcriptomic sequencing reads reported in this paper are available under NCBI's GenBank unifying BioProject IDs PRJNA614527 and PRJNA391713 and BioSample IDs SAMN14342334, SAMN07273876, SAMN07273879, and SAMN07273875. The accession numbers for the individually amplified 18S rRNA gene sequences of *Muranothrix gubernata* (strains MURANO, SUMMARTIN, and RIDKA), *Thigmothrix strigosa* (strains TANZMANG, BALOS2, EBRO3MU, FRESHMU, F1CIIMU, WH5MU, JUD8LAMU, and 11BMUSALTG), *Parablepharisma* sp. (strains SALTPOND, 10BSIPPRAB, 7BFRESHRIV, SALT5CPA, WH5PA, and SALT20PA), and metopid sp. SK (strain SK) reported in this paper are GenBank: MT177189, MT177190, MT177191, MT177192, MT177193, MT177194, MT177195, MT177196, MT177197, MT177198, MT177199, MT177200, MT177201, MT177202, MT177203, MT177204, MT177205, and MT231936. Original data (single gene trees datasets for phylogenomic analyses, protein datasets for mitochondrial pathway prediction, and annotated mitogenomes) have been deposited to DRYAD: https://doi.org/10.5061/dryad.vx0k6djnm. All other information on accessing data analyzed in this study is included in the manuscript or in the Supplemental Information.

EXPERIMENTAL MODEL AND SUBJECT DETAILS

Formal Treatment of New Taxa and Taxonomic Summary

New taxa Muranotrichea cl. nov., Muranotrichida ord. nov., Muranotrichidae fam. nov., *Muranothrix* gen. nov., *Muranothrix gubernata* sp. nov., *Thigmothrix* gen. nov., *Thigmothrix strigosa* sp. nov., Parablepharismea cl. nov., and Parablepharismida ord. nov. were described. A full taxonomic summary and diagnoses for the newly described taxa can be found in Data S1 with ZooBank identifiers and inventory numbers for type material also included in Key Resources Table.

Biological Samples and Cultivation of Organisms

All studied strains were isolated from marine, brackish or freshwater sediments (see Table S1) and subsequently maintained in long-term monoprotist or mixed cultures (usually with archamoebae, breviates, preaxostylids, heteroloboseans or other anaerobic protists present in minority) with unidentified bacteria following method described in [28]. The cultures were established by inoculating 1–3 mL of the sample sediment into a tube with 10 mL of 5:5 or 9:1 ratio of the ATCC (American Type Culture Collection) Seawater Cereal Grass Media #1525 and Freshwater Cereal Grass Media #802, prepared following standard ATCC instructions. For culture maintenance, 1 mL of the culture was reinoculated into a new tube with 10 mL of the designated media every week.

Cell Processing and Fixation

To study the morphology, ultrastructure of both ciliates and symbionts (see Figure 1), sufficient numbers of cells were manually picked from 1 mL of a thriving culture using glass micropipettes, or, alternatively, 3 mL of a thriving culture were centrifuged for 10 min at 800 g. For protargol staining, picked cells were fixed in 10% NBF (neutral buffered formalin) for 30–60 min. For scanning electron microscopy, picked cells fixed in a solution of 2.5% glutaraldehyde (Polysciences) and osmium tetroxide (1%). For transmission electron microscopy, centrifuged cells were resuspended and fixed in cacodylate buffer with 2.5% glutaraldehyde (Polysciences), then washed three times in 0.1 M cacodylate buffer and postfixed with 2% OsO4 in 0.1 M cacodylate buffer. For fluorescence microscopy detection of symbionts using CARD FISH, about 3 mL of each culture were fixed with 10% NBF (neutral buffered formalin) for cells of *Thigmothrix strigosa* strains BALOS2 and EBRO3MU, *Parablepharisma* sp. strains 7BFRESHRIV, 10BSIPPRAB, and SALTPOND, and with 2% OsO_4 for *T. strigosa* strain TANZMANG and *Muranothrix gubernata* strain SUMMARTIN for 30 min.

METHOD DETAILS

Light and Electron Microscopy

The morphology of living and protargol-impregnated cells (see Figures 1C, 1F, 1H, 1L, 1M, 1P, 1Q, S2A–S2C, and S2H) was examined under an Olympus BX51 microscope equipped with digital camera (Olympus), cell measurements (see Tables S2 and S3) were made using a calibrated software QuickPhoto (Promicra). Differential interference contrast (DIC) and brightfield illumination (BF) were used to observe living and protargol-impregnated cells, respectively. F420 coenzyme autofluorescence, typical for some archaeal methanogens [88], was examined using fluorescent Zeiss Axio Imager M2 (Carl Zeiss AG) outfitted with filter set 05 (Zeiss 488005-0000-000). Color micrographs of symbiont autofluorescence (see Figure 1O) were obtained with a Canon EOS Rebel T2i (Canon Inc.). For protargol staining, cells were processed according to the protocol described by [89] and modified in [28]. Briefly, fixed cells were washed three times with tap water and submerged in 1% 1:1 albumin-glycerol (Mayer's albumin), placed on a glass slide using a glass micropipette and air-dried for at least two h. Dried slides were transferred through 95% ethanol, 70% ethanol, tap water, 0.2% potassium permanganate solution, and 2.5% oxalic acid for standard times described in [88]. Washed three times in tap water and once in distilled water, slides were placed for 20 min in 0.4% protargol solution (Polysciences) pre-warmed at 60°C. After sufficient development in Dieckmann's acetone developer according to [88], slides were transferred through tap water, sodium thiosulfate, tap water, graded ethanol series (70%, 100%, 100%), xylene, and mounted with a coverslip in DPX mounting medium (Sigma – Aldrich). For scanning electron microscopy (SEM), in short, fixed cells were cleaned from debris and installed into brass chambers described in [88], using glass micropipettes, transferred through graded ethanol series (30%, 50%, 70%, 95%, 100%, 100% for 5 min each) to dehydrate, and then processed in Critical Point Dryer (Bal-Tec CPD 030). Dried cells were placed onto adhesive carbon tabs on aluminum stubs, using forceps and a fine brush or an eyelash, and gold-sputtered using Sample Sputter Coater (Bal-Tec SCD 050). Processed samples (see Figures 1A, 1B, 1D, 1E, 1G–1J, 1N, 1R, S2G, and S2L) were examined using JSM-6380 scanning electron microscope (JEOL LV). For transmission electron microscopy, the cells were processed as previously described in [28]. Briefly, fixed cells were washed in distilled water, dehydrated in a graded ethanol series (30%, 50%, 70%, 80%, 90%, 95%, 3 × 100%) and infiltrated with a series of 1:1 ethanol-acetone mixture, 100% acetone, and 1:1 acetone- EPON resin mixture. After, cells were embed in absolute EPON resin (Poly/Bed 812, Polysciences) and polymerized at 70 ◦C for 48 h. Serial ultrathin sections were cut on an Ultracut E ultramicrotome (Reichert) using a diamond knife and stained with lead citrate and uranyl acetate (2%–3%). Sections (see Figures 1U–1X, S2E, S2F, and S2I–S2L) were examined using JEOL 1011 transmission electron microscope (JEOL LV).

Fluorescence Microscopy and CARD-FISH

Catalyzed Reporter Deposition-Fluorescence *In Situ* Hybridization (CARD-FISH) was applied to detect prokaryotic symbionts of the studied organisms (see Figures 1K, 1S, and 1T), using the group specific probes DELTA495abc and competitor cDELTA495abc, specific to most delta-proteobacteria [76], and ARC915, specific to most archaea [75], according to the protocol by [90] modified in [30]. Fixed ciliate cells were filtered on 10 μm pore size, 25cmm Isopore GTTP filter (Millipore, Billerica) and rinsed three times with 5 ml sterile phosphate-buffered saline (PBS). After air-drying, filter sections were embedded with 37°C 0.2% (w/v) MetaPhor agarose (Lonza) and dried at 46°C. To inactivate the endogenous peroxidases, filter sections were incubated in 10 ml of 0.01 M HCl for 10 min at room temperature and subsequently rinsed in 50 ml 1 × PBS, followed by washing in deionized sterile water. Permeabilization of prokaryotic cells was conducted in a lysozyme solution (10 mg/ml Lysozyme; 0.05 M EDTA; 0.1 M Tris-HCl, pH 8) at 37°C for 60 min and washing in deionized sterile water and absolute ethanol. For both DELTA495abc and ARC915 probes, the hybridization was carried out at 46°C for 2.5 h in a 100:1 mix of Hybridization Buffer (35% formamide). Filter sections were rinsed in washing buffer (5 mM EDTA; 20 mM Tris-HCl, pH8; 70 mM NaCl; 0.01% SDS) for 5 min at 48°C, then incubated 15 min at room temperature in PBS 1X. For signal amplification with catalyzed reporter deposition, filter sections were incubated for 15 min at 37°C in a mix of amplification buffer (1 × PBS, 0.1% Blocking Reagent, 2 M NaCl and 0.1 g/ml dextran sulfate), H_2O_2 (0.015%) and the fluorescently labeled tyramide Alexa488 (Biomers.net GmbH), and then washed twice in 1X PBS, once in deionized sterile water and once in absolute ethanol. After air-drying, filter sections were mounted onto microscope slides with a drop of solution prepared from 1571 μL Citifluor (Citifluor Ltd.); 286 μL VectaShield with DAPI (Vector Laboratories); 143 μL 1 × PBS. Slides were observed using a Zeiss Axio Imager M2 microscope equipped with a Zeiss AxioCam camera (Carl Zeiss Microscopy GmbH). Ciliate nuclei were detected under DAPI-excitation fluorescence (350 nm), and CARD-FISH targeted prokaryotic cells under GFP-excitation (500 nm) epifluorescence.

DNA/RNA Extraction, Amplification, and Library Preparations

Genomic DNA from each studied ciliate strain (see Table S1) was isolated as follows: after 1.5 mL of each culture were centrifuged for 10 minutes at 800 g, 1.4 mL of the supernatant was removed and the remaining 100 μL was resuspended and used for DNA isolation, using a DNA isolation kit (Genomic DNA Minikit, Geneaid; DNeasy Blood & Tissue Kit, QIAGEN; or ZR Genomic DNA Kit II TM, Zymo Research) according to the manufacturer's instructions. The DNA was stored at −20°C until processed. The 18S rRNA gene was amplified with primers designed for eukaryotes [77], MedA (5′-AACCTGGTTGATCCTGCCAGT-3′) and MedB (5′TGATCCT GCAGGTTCACCTAC-3′) and an annealing temperature of 60°C. In most cases, direct sequencing of PCR products was possible but in cases with several related ciliate strains present in the culture, selected strains were cloned to obtain the desired sequence, using the pGEM-T Easy Vector System I (Promega) and JM109 competent cells of *Escherichia coli* (High Efficiency Competent Cells, Promega). For metagenomic DNA isolation, approximately 60 cells of *Parablepharisma* sp. SALTPOND and metopid sp. SK strains

(see Table S1) were hand-picked from cultures with a drawn glass Pasteur pipette, starved for 2–3 h to reduce the contribution of prey organisms to metagenomic sequences, washed in sterile water and deposited into UV-sterilized DNA/RNAShield (Zymo Research Corp.), as described for *Heterometopus* sp. CSS metagenome DNA isolation used for its symbiont genome analysis in [66]. In addition, metagenomic DNA from a centrifuged and resuspended pelet of about 0.5 L of monoeukaryotic culture of *Muranothrix gubernata* SUMMARTIN, filtered from prokaryotes using 5 μm isopore filters (MilliPore), was extracted using Genomic DNA Minikit (Geneaid). Total RNA from *Muranothrix gubernata* SUMMARTIN was extracted from approximately 0.5 l of well-grown monoeukaryotic cultures using TriReagent (Sigma – Aldrich), purified using the RNeasy mini kit (QIAGEN), and treated with DNase (QIAGEN). Followingly, mRNA was selected from total RNA using the Dynabeads Oligo(dT) 25 system (ThermoFisher Scientific). A bacterial rRNA depletion step using the RiboMinus kit (ThermoFisher Scientific) was added. An RNA-seq library was prepared by the EMBL Genomics Core Facility (GeneCore), Heidelberg, Germany. Data from each library was cross-checked to confirm species identity of the sequenced culture. Raw pair-end reads were merged using the program PEAR (http://sco.h-its.org/exelixis/web/software/pear/doc.html).

Sanger Sequencing and Illumina NextSeq Sequencing

Sanger sequencing of rRNA genes was done with an ABI PRISM 3100 sequencer (ThermoFisher Scientific) at the Laboratory of DNA sequencing at Charles University, Prague, Czech Republic. Metagenomes were sequenced from the picked cells and a culture using Illumina NextSeq (Illumina Inc.) (150-bp paired-end reads, 300-bp insert size) as described in [66]. Transcriptome was sequenced by EMBL Genomics Core Facility (GeneCore), Heidelberg, Germany.

Metagenomic and Transcriptomic Assemblies

For metagenomes, Trimmomatic v0.36 [78] was used to filter and trim paired reads from all samples. Filtered and trimmed reads were then combined and co-assembled with IDBA-UD v.1.1.1 [91]. Metagenomic contigs > 1 kb were binned using CONCOCT [92] as implemented in Anvi'o v2.0.3 [93], which bins contigs based on nucleotide composition and differential coverage data from mapping reads to the co-assembly. The reads mapping to an affiliated genomic bin of each target ciliate from the initial binning results were re-assembled with IDBA-UD v.1.1.1 [91] to improve bin quality. CheckM [94] was used to evaluate the completeness, contamination, and taxonomy of genomic bins, as well as to identify rRNA gene sequences. Additional metagenomic reads from *Muranothrix gubernata* SUMMARTIN, sequenced subsequently in order to obtain mitochondrial genome from Muranotrichea, were quality trimmed using Trimmomatic v0.39, corrected by Rcorrector and assembled using Metaspades (SPAdes genome assembler v3.13.1) with default settings for paired-end reads in "only-assembler" mode. Contigs representing mitogenomes were identified in metagenome assemblies by BLAST using available protein sequences from ciliate mitogenomes as a query (GenBank: GU057832.1, JN383843.1, and NC_014262.1). Subsequently, we used manual approach based on iterative searches in Illumina reads (BLASTN) followed by read alignment to the corresponding contig (Geneious Prime; "map to reference" option) to unambiguously extend the longest *Parablepharisma* sp. mitogenome fragment. This resulted in 41,931 bp long sequence (opposed to original contig length 35,877 bp). Initial annotations of mitogenome sequences were obtained using MFannot (online version from October 23, 2019). Predicted genes recovered by MFannot (including hypothetical proteins) were individually checked to confirm/reveal their identity and to exclude possible bacterial contamination using BLAST against the nr GenBank database. Graphical genome maps were produced by OrganellarGenomeDRAW (OGDRAW) v1.3.1 [79]. For transcriptomic data, quality trimming and Illumina adaptor and sequence contamination removal was done using the program Trimmomatic [78]. Transcriptomes were assembled using the software package Trinity [95].

Datasets preparation and rRNA gene phylogenetic analyses

Two datasets, containing 18S rRNA gene sequences/18S and 28S rRNA gene sequences concatenated using Mesquite [96], consisted of 17/2 newly determined sequences of Muranotrichea and Parablepharismea (see Table S1), 1/2 newly determined and 24/0 GenBank sequences of Metopida (Armophorea), 12/1 GenBank sequences of Clevelandellida (Armophorea), 3/0 GenBank sequences of Armophorida (Armophorea), 8/6 GenBank sequences of Litostomatea, 28/31 GenBank sequences of Spirotrichea *sensu lato*, 2/1 GenBank sequences of Odontostomatea, 1/0 GenBank sequence of Cariacotrichea, and 41/41 GenBank sequences of other ciliates (CONThreeP, Protocruziiea, Heterotrichea, Karyorelictea) used as outgroup. Two environmental sequences (Genbank: KT346287 and KT346288 [87]), affiliated as related to the newly described taxa by BLAST, were excluded from the analyses due to chimeric origin. The sequences were aligned using MAFFT [85] on the MAFFT 7 server (http://mafft.cbrc.jp/alignment/server/) with L-INS-i algorithm and default settings. The alignments were manually checked for chimeras and edited using BioEdit 7.0.9.0 [80]. 18S rRNA, and concatenated 18S and 28S rRNA phylogenetic trees were constructed by maximum likelihood (ML) and Bayesian analyses. ML analyses were performed in RAxML 8.0.0 [81] under the GTRGAMMAI model with 1000 rapid bootstraps. Node support was assessed by ML analysis of 1000 bootstrap datasets. Bayesian analyses were performed using Phylobayes [84] with GTR CAT. For 18S rRNA gene, four independent chains were run for 34,720 generations (maxdiff = 0.0531, 20% burnin). For concatenated 18S and 28S rRNA genes, four independent chains were run for 150,000 generations (maxdiff = 0.14, 20% burnin).

Phylogenomic analyses

Extensive phylogenomic datasets of ciliates [24, 74], containing ~160 and 124 genes, respectively, were used as reference datasets. Procedures outlined in [64] and [23] were followed. In brief, up to five best hits were recovered (E-value < 1E-5) for each gene

from the *Muranothrix* transcriptome using BLAST and translated into protein sequences using the Barrel-O-Monkeys package (http://rogerlab.biochemistryandmolecularbiology.dal.ca/monkeybarrel.php). In the case of metagenomes, genes of interest were recovered using in-house script (https://github.com/DavidZihala/raw_gene_prediction?fbclid=IwAR2xbkMEUe8Fvl2A_6uJF2r4oT9IJWx7iopVQMxjqgows5VcxsXTYCi5IP8). Each recovered sequence was then reciprocally blasted against reference datasets enriched with well-defined known paralogs (e.g., EF-1α and EFL) to assist in the identification and removal of deep-paralogs. BLAST searches against the Swissprot database was used to trim away non-homologous sequence data at the end of predicted genes. Subsequently, all sequences were added to single-gene alignments. These were then aligned using the MAFFT-LINSI algorithm (with default parameters), trimmed in BMGE [86] (gap threshold set to 0.3) and single gene trees were reconstructed using RAxML [81] (model setting PROTGAMMALGF) with 100 rapid bootstraps. Single gene trees were then investigated by eye and proper orthologs were selected from targeted taxa, while putative paralogs were removed, creating final version of the single gene datasets (available at DRYAD: https://doi.org/10.5061/dryad.vx0k6djnm). Each single gene dataset was then aligned by MAFFT LINSI algorithm [85] (with default parameters), followed by trimming using BMGE v 1.2 [86] (gap threshold set to 0.3). Trimmed alignments were then concatenated into one super-matrix using the program alvert from the Barrel-O-Monkeys package. The maximum likelihood phylogenomic tree was constructed in IqTree [82] using the C40+LG+F+G model with 1000 PMSF [83] bootstraps. Bayesian analysis was performed using Phylobayes [84] with CAT-GTR+G with constant sites removed. Four independent chains were run for 16,000 generations (maxdiff = 0.002, 20% burnin).

In-silico predictions of mitochondrial metabolism

Genes of interests were collected from previously published studies of anaerobic mitochondria [4, 6, 7, 17, 18] and from the published mitochondrial proteome of *Tetrahymena thermophila* [35]. Candidate sequences from ciliates were recovered by blast and hits with e-value < 1e-10 were extracted and added to the initial datasets for each gene (see Data S2). Published datasets [7] were used as starting datasets, where available. When a published dataset was not available, starting datasets were constructed by blast searches of a seed sequence against nr (max target seqs = 100). Additionally, sequences from taxonomically diverse eukaryotic and prokaryotic representatives identified through searches of the gene name in NCBI protein and RefSeq databases. The resulting sequences were combined into a single dataset and clustered in CD-Hit at 75% [97]. Each gene dataset was aligned using MAFFT-LINSI (default settings), trimmed using trimal (gappyout) and trees were constructed using RAxML (PROTGAMMALG with 100 rapid bootstraps). Each alignment/tree has been repeatedly inspected by eye and sequences were added/removed as necessary. Each tree was then manually evaluated for presence absence of genes of interest in studied lineages (see Data S2).

QUANTIFICATION AND STATISTICAL ANALYSIS

Statistical support for the phylogenomic tree (Figure 2A) was inferred from 1000 bootstrap replicates using the LG+C40+G4+F PMSF profiles in program IqTree [82]. Posterior probabilities were inferred from four independent chains using program Phylobayes [84] (CAT-GTR+G model, 16,000 generations (maxdiff = 0.002, 20% burnin). Statistical support for single gene phylogenetic trees (Data S2) and rRNA gene phylogenetic trees (Figures 2C and S1) was inferred using 100 and 1000 rapid bootstraps in RAxML 8.0.0 [81] under models LG+G and GTRGAMMAI, respectively. Morphometric cell measurements and counts (Tables S2 and S3) were made from digital images using calibrated software QuickPhoto (Promicra) or using ocular micrometer. Coefficients of variation, medians, minimum and maximum values, arithmetic means, and standard deviations of the arithmetic mean in Tables S2 and S3 were assessed using the Descriptive Statistics platform (http://home.ubalt.edu/ntsbarsh/Business-stat/otherapplets/Descriptive.htm).